

# Nonlinear magnetohydrodynamics theory

&

## HPC physics

Marco Veranda

[marco.veranda@igi.cnr.it](mailto:marco.veranda@igi.cnr.it)

*Consorzio RFX (CNR, ENEA, INFN, Università di Padova, Acciaierie Venete SpA)  
CNR, Istituto per la Scienza e la Tecnologia dei Plasmi*

Padova, Italy

November 26<sup>th</sup> 2024

# OUTLINE of the lesson

- Intro: meaning of nonlinearity, why it is necessary to deal with it;
- Basics: recap of MHD models
- example 1: magnetic reconnection
- example 2: sawtoothing in tokamaks
- HPC physics (and programming techniques)

# why nonlinearity is difficult

- Most nonlinear systems are impossible to solve analytically. Why are nonlinear systems so much harder to analyze than linear ones?
- The essential difference is that linear systems can be broken down into parts. Then each part can be solved separately and finally recombined to get the answer. This idea allows a fantastic simplification of complex problems, and underlies such methods as normal modes, Laplace transforms, Fourier analysis and the superposition principle.
- In this sense, **a linear system is precisely equal to the sum of its parts.**
- But many things in nature don't act this way. Whenever parts of a system interfere, or cooperate, or compete, there are nonlinear interactions going on.
- Most of everyday life is nonlinear, and the principle of superposition fails spectacularly (try to listen to your two favorite songs at the same time, you won't get double the pleasure!)
- Within the realm of physics, nonlinearity is vital to the operation of a laser, the formation of turbulence in a fluid, and the superconductivity of Josephson junctions, just to write the first phenomena coming to my mind.

quotes from Steven H. Strogatz, Nonlinear dynamics and Chaos, 2015, Westview Press

# speaking with equations

- linear differential equation of order n

$$a_n(x) \frac{d^n y(x)}{dx^n} + a_{n-1}(x) \frac{d^{n-1} y(x)}{dx^{n-1}} + \cdots + a_1(x) \frac{dy(x)}{dx} + a_0(x)y(x) = f(x)$$

- $y(x)$  cannot have powers higher than 1, i.e. no  $y(x)^2$ , and multiplication of derivatives  $\frac{dy}{dx} \cdot \frac{d^3y}{dx^3}$ , or be contained in nonlinear functions (no  $\ln(y)$ ).
- superposition principle: if  $y_1(x)$  and  $y_2(x)$  are solutions, then also  $ay_1(x) + by_2(x)$  is a solution of the differential equation (i.e. it can create a vector space, very useful)
- nonlinear differential equation of order n

$$a_n(x) \color{orange}y(x)\color{black} \frac{d^n y(x)}{dx^n} + a_{n-1}(x) \color{orange}\sin(y(x))\color{black} \frac{d^{n-1} y(x)}{dx^{n-1}} + a_1(x) \color{orange}\frac{dy(x)}{dx} \color{black} \frac{dy(x)}{dx} + a_0(x)y(x) = f(x)$$



# What is and why we need a nonlinear exploration of the MHD model for plasmas

- MHD describes the macroscopic behaviour of electrically conducting fluids, i.e. a plasma;
- Since the first studies in the 1950s, equilibrium and stability have been widely tackled:
  - equilibrium state is separated from small perturbations, linear MHD;

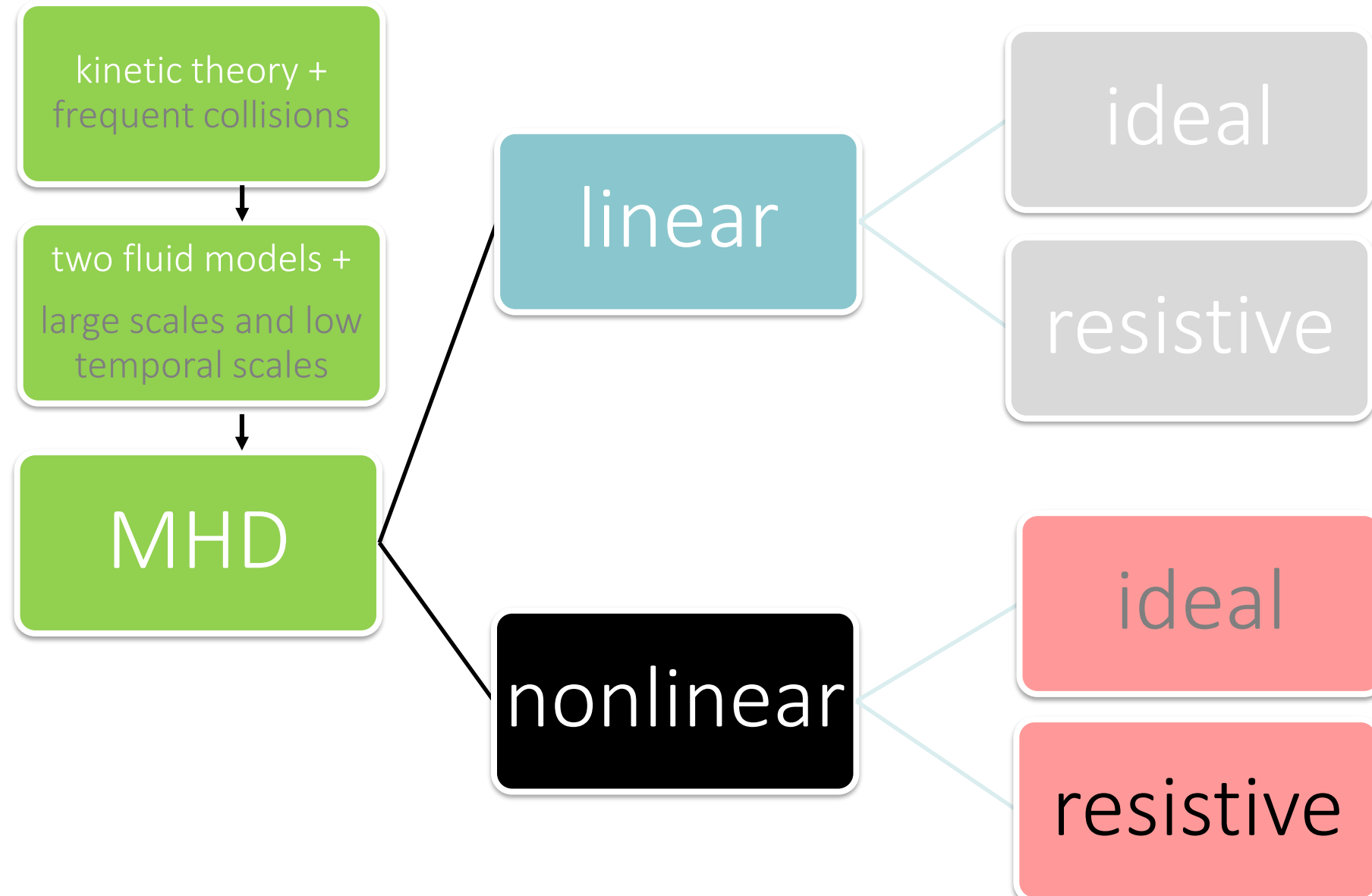
# Linear / quasi linear / nonlinear approaches

- Linear picture: instability would lead to the destruction of the equilibrium configuration and loss of the plasma confinement.
- Linear dynamics is a very important tool, but it is insufficient to predict the final state of unstable dynamics in various types of disrupted processes routinely observed in magnetically confined fusion plasmas
- necessity to consider nonlinear dynamics
- Plasma discharges in reality exist even if instabilities are present → need to compute nonlinear behaviour or, at least, saturation levels.
- The most privileged approach would be to follow the nonlinear development from an unstable equilibrium;

# Linear / quasi linear / nonlinear approaches

- POSSIBLE APPROACHES:
  - study slowly evolving equilibrium states (ideal kink mode, resistive kink, asymptotic states of system relaxed under some constraints);
  - Fully developed MHD turbulence (averages);
  - numerical computations: problem is considered solved if “scaling laws” can be obtained.
- But also QUASI-LINEAR theory: only take into account the action of the unstable modes on the equilibrium profiles.

# a diagram about possible modelling of hot plasmas



# 3D nonlinear resistive MHD equations

$$\frac{\partial \rho}{\partial t} + \nabla \cdot (\rho \mathbf{v}) = 0$$

mass continuity equation

$$\rho \frac{\partial \mathbf{v}}{\partial t} + \rho \mathbf{v} \cdot \nabla \mathbf{v} = \mathbf{J} \times \mathbf{B} - \nabla p$$

momentum equation

$$\frac{\partial p}{\partial t} + \mathbf{v} \cdot \nabla p + \gamma p \nabla \cdot \mathbf{v} = (1 - \gamma) \eta J^2$$

energy equation

$$\frac{\partial \mathbf{B}}{\partial t} = -\nabla \times \mathbf{E}$$

Faraday equation

$$\mathbf{E} + \mathbf{v} \times \mathbf{B} = \eta \mathbf{J}$$

Ohm equation

$$\nabla \times \mathbf{B} = \mu_0 \mathbf{J}$$

Ampère equation

$$\nabla \cdot \mathbf{B} = 0$$

Gauss equation

# Model equations: fundamental time scales

- by studying the linearized small-amplitude oscillatory solution of the MHD model (theory of *MHD waves*, it would require a lesson on its own) the fundamental temporal and velocity scales emerge:

$$\text{Alfvén velocity } v_A \equiv \frac{B_0}{\sqrt{\mu_0 \rho_0}}$$

and, by assuming a macroscopic lenght of the system  $L$  one gets the Alfvén time  $\tau_A = \frac{L}{v_A}$

- By rewriting the equations of slide 6 normalizing all quantities to the Alfvén velocity and time and to the macroscopic length one can obtain the

$$\text{resistive time scale } \tau_R = \frac{\mu_0 L^2}{\eta}$$

# resistive MHD: basics / timescales involved

- Faraday equation + Ohm's law for a plasma:

$$\frac{\partial \mathbf{B}}{\partial t} = -\nabla \times \mathbf{E} \quad \text{and} \quad \mathbf{E} + \mathbf{v} \times \mathbf{B} = \eta \mathbf{J} \quad \text{and} \quad \nabla \times \mathbf{B} = \mu_0 \mathbf{J}$$

- interesting fact: Ohm's law is similar to the one valid in electromagnetism, only the electric field is replaced by an effective one  $\mathbf{E} + \mathbf{v} \times \mathbf{B}$ , the effective electric field seen by a fluid element moving with velocity  $\mathbf{v}$  across a magnetic field  $\mathbf{B}$ , taking into account the Lorentz transformation for  $v \ll c$ .

$$\frac{\partial \mathbf{B}}{\partial t} = \nabla \times \left( \mathbf{v} \times \mathbf{B} - \frac{\eta}{\mu_0} \nabla \times \mathbf{B} \right) = \color{orange} \nabla \times (\mathbf{v} \times \mathbf{B}) - \frac{\nabla \eta}{\mu_0} \times \nabla \times \mathbf{B} + \color{orange} \frac{\eta}{\mu_0} \nabla^2 \mathbf{B}$$

- assume uniform resistivity and compare the two terms:

$$\frac{|\nabla \times (\mathbf{v} \times \mathbf{B})|}{\left| \frac{\eta}{\mu_0} \nabla^2 \mathbf{B} \right|} = \frac{v B \mu_0 L^2}{L \eta B} = \frac{\mu_0 L v}{\eta} = Re_M$$

def:  $\tau_R \equiv \frac{\mu_0 L^2}{\eta}$

( $Re_M$ : magnetic Reynolds number)

- upper bound:  $v \sim v_A$ , Lundquist number  $S = \frac{\tau_R}{\tau_A} = \frac{\mu_0 L v_A}{\eta}$

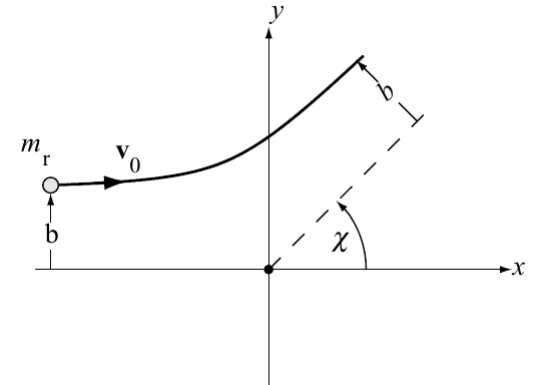
# resistive MHD: basics / remind of Spitzer's formula for the resistivity of a plasma

- Lundquist number  $S = \frac{\tau_R}{\tau_A} = \frac{\mu_0 L v_A}{\eta}$
- due to charged particles "collisions" (semantics);
- dependence on the typical time scale of electron-ion collision frequency;

$$\eta = \frac{0.06 e^2 m_e^{1/2}}{\pi^{3/2} \epsilon_0^2} \frac{\ln \Lambda}{T_e^{3/2}}$$

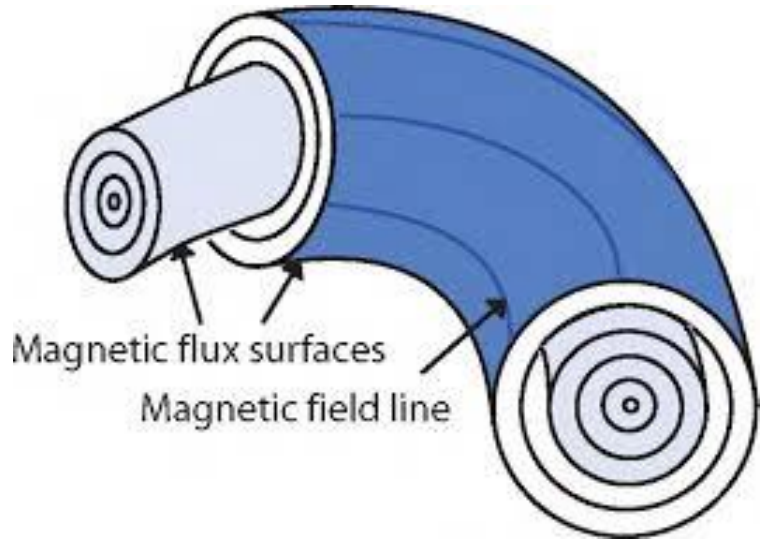
all units in SI, temperature in [J]

- Coulomb logarithm  $\ln \Lambda$  contains details about the close encounters between an electron and an ion, and it is practically constant for fusion plasmas  $\ln \Lambda \sim 15$
- in hot fusion plasmas  $S \sim 10^6 - 10^9$

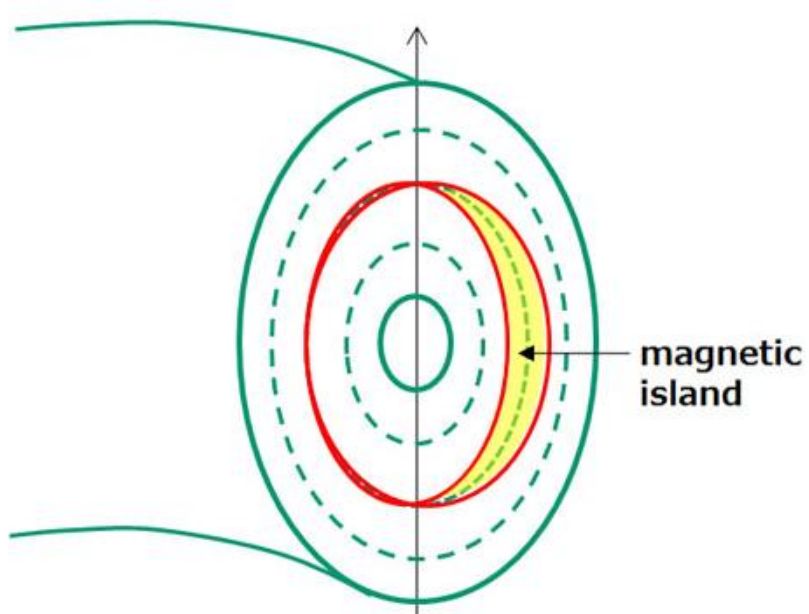


REF: chapter 9 of J. Freidberg, Plasma Physics and Fusion Energy, Cambridge University Press 2007

# ideal vs resistive MHD



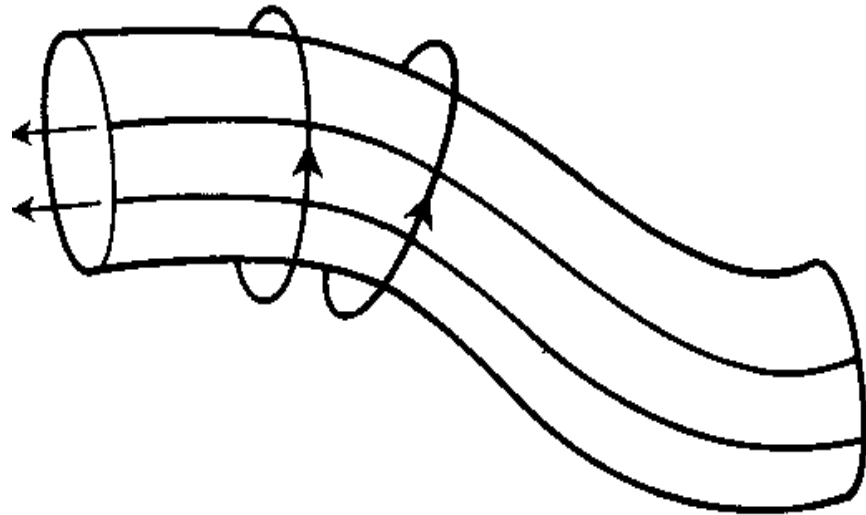
Ideal MHD:  $\eta = 0$   
**flux conservation inside a magnetic flux surface\***  
**topology unchanged**



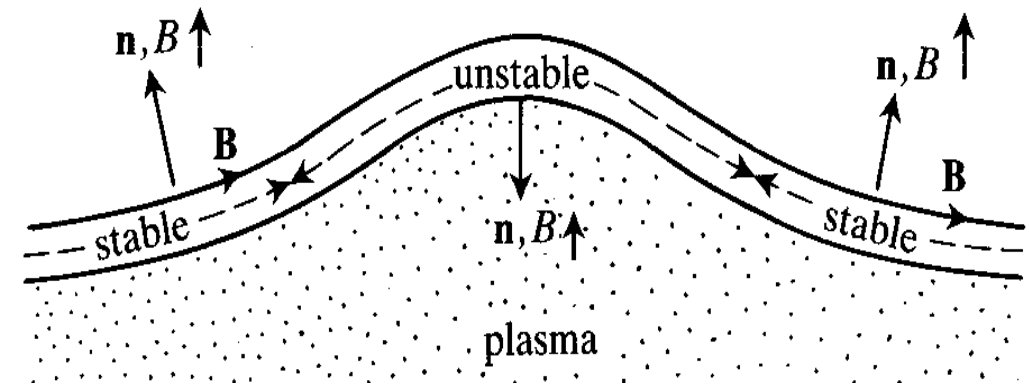
Resistive MHD:  $\eta \neq 0$   
**reconnection of field lines**  
**topology changes**

\*the lines of force of the magnetic field are ‘frozen’ in the plasma if ideal MHD holds. Indeed, in ideal MHD (perfect conductivity!), the concept of magnetic field lines obtains more physical reality than it even had in Faraday’s times. cfr. Alfvén theorem.

# Free energies to drive MHD modes



current driven instabilities  
(kink / tearing modes)



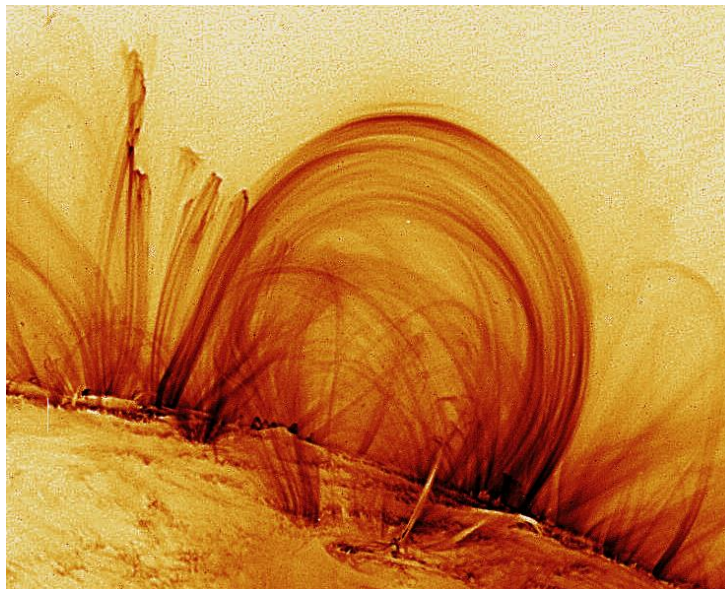
pressure driven instabilities  
(interchange mode)

## two cases (between many, not exhaustive)

- 1) Magnetic reconnection / resistive-kink tearing modes dynamics in resistive MHD
- 2) Sawtoothing in tokamaks / nonlinear cycles

# magnetic reconnection

- Magnetic reconnection is a change of connections of magnetic field lines in highly conducting plasmas. A modification of the magnetic field topology results<sup>1</sup>.
- Magnetic reconnection is a common phenomenon in space and laboratory plasmas: it is found in solar flares<sup>2</sup>, jets from active galactic nuclei<sup>3</sup>, strongly magnetized neutron stars<sup>4</sup>, astrophysical dynamos<sup>5</sup>, large-scale magnetic self-organization of toroidal plasmas for magnetic fusion experiments<sup>6</sup>.



[http://soi.stanford.edu/results/SolPhys200/Schrijver/images/loops\\_6nov99b.gif](http://soi.stanford.edu/results/SolPhys200/Schrijver/images/loops_6nov99b.gif)

coronal loops over the eastern limb of the Sun was taken in the TRACE 171Å pass band, characteristic of plasma at 1 MK, on November 6, 1999, at 02:30 UT

## MINIMAL BIBLIOGRAPHY ABOUT MAGNETIC RECONNECTION

1 Yamada M, Kulsrud R, Ji H (2010) Magnetic reconnection. Rev Mod Phys 82:603–664.

2 Innes D, Inhester B, Axford W, Wilhelm K (1997) Bi-directional plasma jets produced by magnetic reconnection on the sun. Nature 368:811

3 Romanova MM, Lovelace RVE (1992) Magnetic field, reconnection and particle acceleration in extragalactic jets. Astron Astrophys 262:26–36

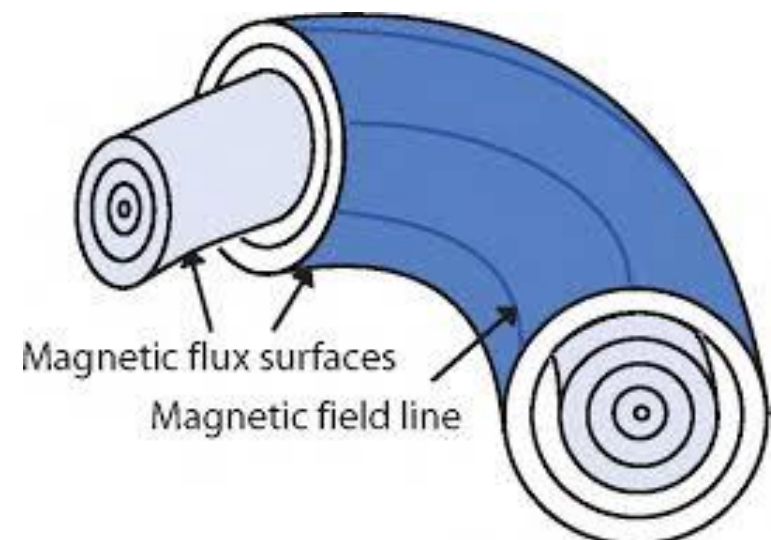
4 Hurley K, Boggs S, An exceptionally bright flare from sgr1806-20 and the origins of short-duration gamma-ray bursts. Nature 434:1098–1103.

5 Plasmas 23(3):032111. <https://doi.org/10.1063/1.4942940> Cowling T (1934) The magnetic field of sunspots. Mon Not R Astron Soc 94:39

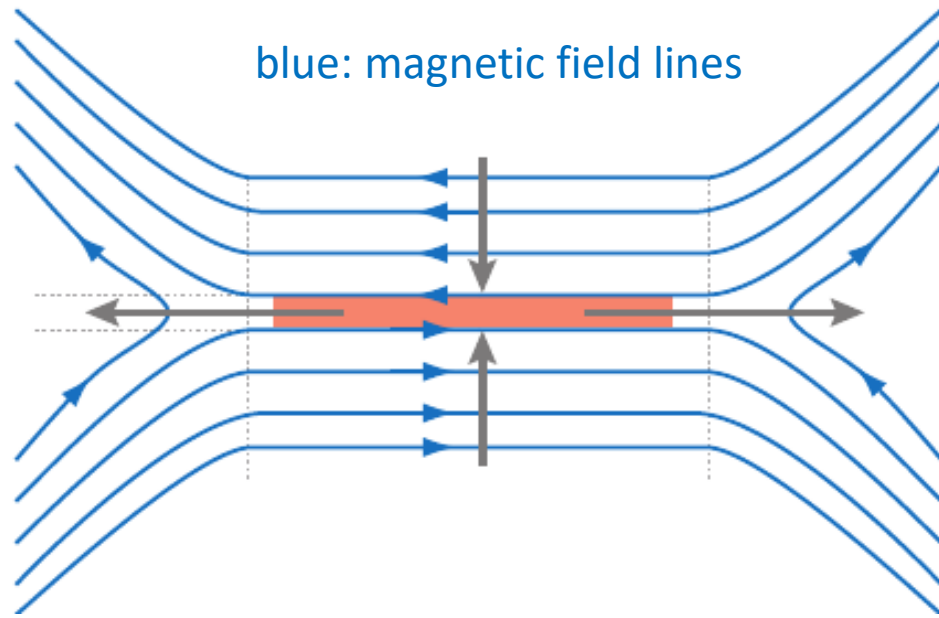
6 Taylor J (1974) Relaxation of toroidal plasma and generation of reversed magnetic fields. Phys Rev Lett 33(19):1139

# magnetic reconnection

- Magnetic reconnection is a change of connections of magnetic field lines in highly conducting plasmas. A modification of the magnetic field topology results<sup>1</sup>.
- Magnetic reconnection is a common phenomenon in space and laboratory plasmas: it is found in solar flares<sup>2</sup>, jets from active galactic nuclei<sup>3</sup> strongly magnetized neutron stars<sup>4</sup> astrophysical dynamos<sup>5</sup> large-scale magnetic self-organization of toroidal plasmas for magnetic fusion experiments<sup>6</sup>.
- A common signature of magnetic reconnection is the release of magnetic energy, converted into kinetic and thermal internal energy of the plasma, and observed as acceleration of particles to non-thermal velocities, and as generation of waves and turbulence. Another signature of reconnection is the presence of so-called current sheets.
- In toroidal experiments for magnetic confinement of fusion plasmas, reconnection is generally linked to the opening of “islands” in the field lines topology. For optimum confinement magnetic field lines should lie on nested magnetic flux surfaces (which means existence of a function  $\chi$  such that  $\mathbf{B} \cdot \nabla \chi = 0$ , with the shape of a topological torus).
- However, such magnetic fields can be unstable in the vicinity of the regions where field lines close on themselves, and a transverse component of the magnetic field opens the magnetic islands, bounded by a so-called separatrix containing a region with “X” topology.

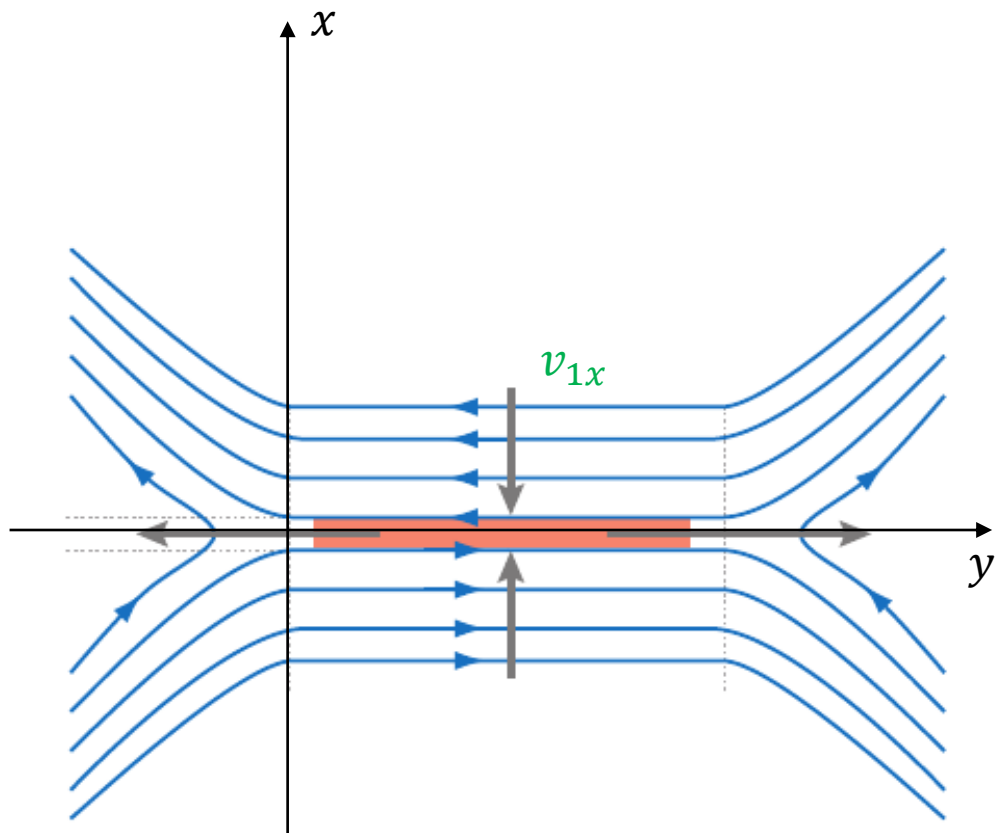


# the basic model of magnetic reconnection



basic picture: two magnetic field lines being carried by the fluid come closer together and by the action of resistivity they are cut and reconnected in a different topology

# simplest model to study reconnection: Sweet - Parker



$$\frac{\partial \mathbf{B}}{\partial t} = \nabla \times (\mathbf{v} \times \mathbf{B} - \eta \mathbf{J})$$

if  $\partial_t \mathbf{B} = 0$  then

$$\mathbf{J} = \frac{1}{\eta} \mathbf{v} \times \mathbf{B}$$

- current sheet at  $x \sim 0$  (because  $\mathbf{B}$  changes direction)
- unstable system, the sheet tends to be levelled by the plasma
- but not in ideal MHD!
- Imagine a force trying to compress the plasma towards  $x = 0$ . Imagine that the plasma moves across magnetic field lines without changing  $\mathbf{B}$  (thus violating ideal MHD) with velocity  $v_{1x}$ : this would create an induced electric field and, using Ohm's law, a current  $J_{1z} = \frac{1}{\eta} v_{1x} B_{0y}$ .
- This would lead to a restoring  $\mathbf{J} \times \mathbf{B}$  force
- $F_x = \frac{1}{\eta} v_{1x} B_{0y}^2$ : infinite if  $\eta \rightarrow 0$  (i.e. frozen-in flux theorem),
- but also  $F_x \sim 0$  at  $x = 0 \rightarrow$  ideal MHD breaks down there

# Sweet Parker: some basic use of continuity equation and Ohm's law

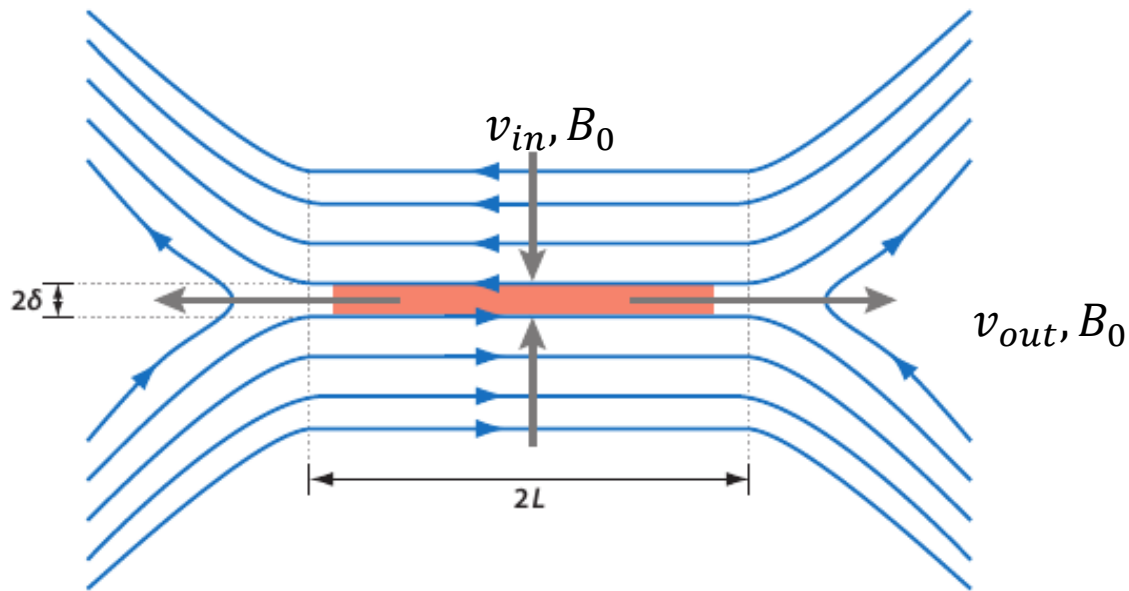


**Figure 1**

Sketch of magnetic field geometry in Sweet-Parker reconnection. Oppositely directed magnetic fields are brought together over a length  $2L$  and reconnect in a diffusion layer of width  $2\delta$ .

- continuity equation:  $v_{in}L = v_{out}\delta$ ;
- consider stationary conditions. Ohm's law:  $E + v_{in}B_0 = \eta J$ : perpendicular to the plane.
- in the **red current sheet** the resistive term dominates,  $E$  negligible:

$$v_{in}B_0 = \eta J = \eta \frac{B_0}{\delta}$$

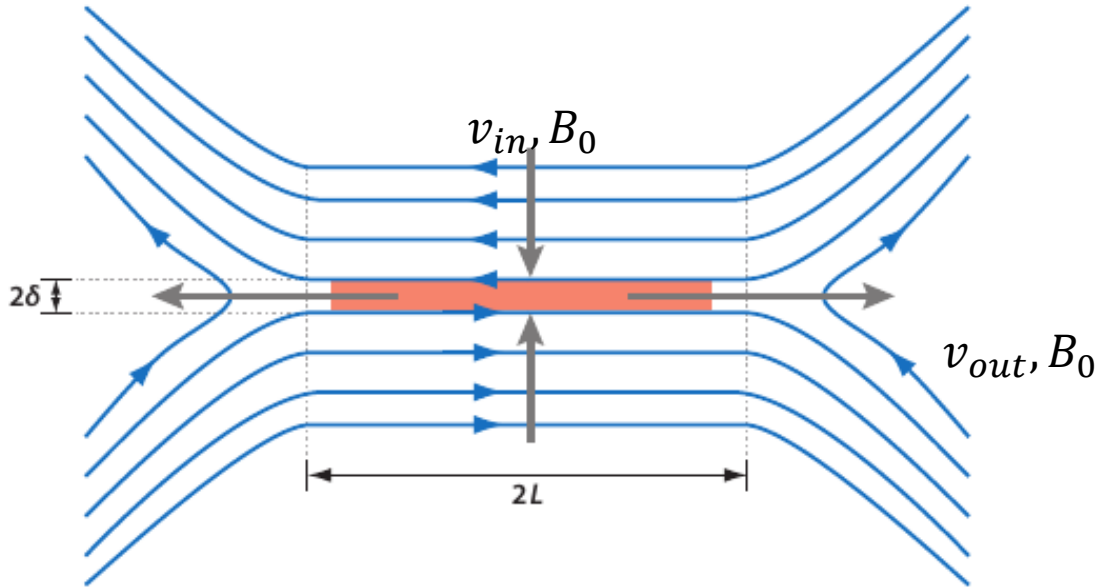


**Figure 1**

Sketch of magnetic field geometry in Sweet-Parker reconnection. Oppositely directed magnetic fields are brought together over a length  $2L$  and reconnect in a diffusion layer of width  $2\delta$ .

- continuity equation:  $v_{in}L = v_{out}\delta$ ;
- $v_{in}B_0 = \eta J = \eta \frac{B_0}{\delta}$
- stationary conditions

$$\frac{\delta}{L} = \frac{v_{in}}{v_{out}} = \frac{\eta}{\delta v_{out}}$$

$$\frac{\delta^2}{L^3} = \frac{\eta}{L^2 v_{out}}$$

$$\frac{\delta^2}{L^3} = \frac{1}{\tau_R v_{out}}$$

multiply by  $L^{-2}$

$$\tau_R \sim \frac{L^2}{\eta}$$

# Sweet Parker: force balance equation

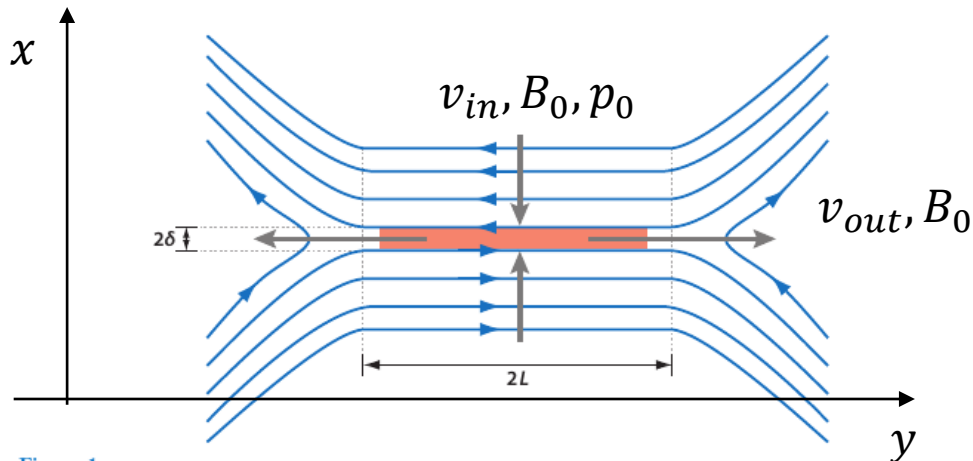


Figure 1

Sketch of magnetic field geometry in Sweet-Parker reconnection. Oppositely directed magnetic fields are brought together over a length  $2L$  and reconnect in a diffusion layer of width  $2\delta$ .

$$\frac{\delta}{L} = \frac{v_{in}}{v_{out}} = \frac{\eta}{\delta v_{out}}$$

$$\frac{\delta^2}{L^3} = \frac{\eta}{L^2 v_{out}}$$

$$\frac{\delta^2}{L^3} = \frac{1}{\tau_R v_{out}}$$

force balance along vertical x direction:

$$\frac{d\mathbf{v}}{dt} = -\nabla p + \mathbf{J} \times \mathbf{B} \Big|_x$$

neglect inertial term

$$-\partial_x p + \nabla \times \mathbf{B} \times \mathbf{B} \Big|_x = 0$$

$$-\partial_x p + (-\nabla \mathbf{B} \mathbf{B} + (\mathbf{B} \cdot \nabla) \mathbf{B}) \Big|_x = 0$$

$$-\partial_x p + B \partial_x B = 0$$

$$\partial_x \left( \frac{B^2}{2} - p \right) = 0$$

integrate from the center,  
where  $B = 0$  and  $p = p_m$  to the outside where  
 $B = B_0$  and  $p = p_0$

$$\frac{B_0^2}{2} = p_m - p_0$$

# Sweet Parker: force balance equation

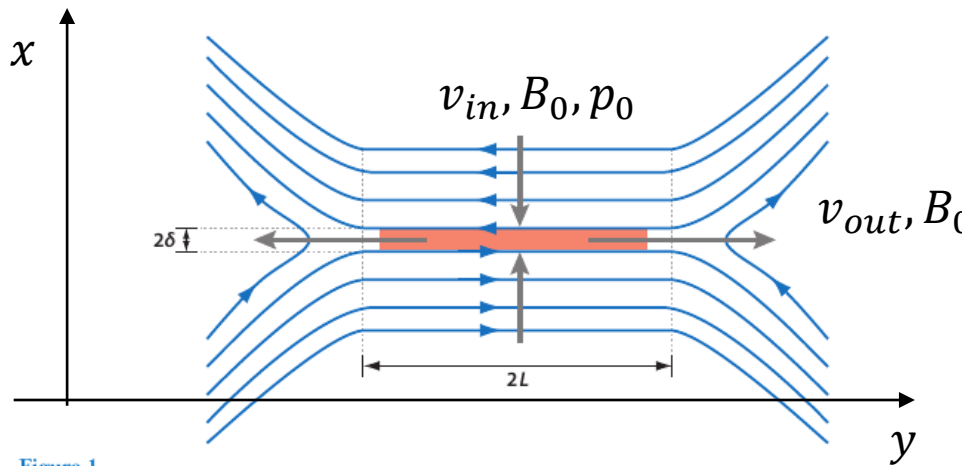


Figure 1

Sketch of magnetic field geometry in Sweet-Parker reconnection. Oppositely directed magnetic fields are brought together over a length  $2L$  and reconnect in a diffusion layer of width  $2\delta$ .

$$\frac{\delta}{L} = \frac{v_{in}}{v_{out}} = \frac{\eta}{\delta v_{out}}$$

$$\frac{\delta^2}{L^3} = \frac{\eta}{L^2 v_{out}}$$

$$\frac{\delta^2}{L^3} = \frac{1}{\tau_R v_{out}}$$

force balance along horizontal  $y$  direction, where  $\mathbf{B}$  vanishes

$$\frac{d\mathbf{v}}{dt} = -\nabla p + \mathbf{J} \times \mathbf{B} \Big|_y$$

$$\mathbf{v}_y \cdot \nabla v_y = -\partial_y p$$

$$\partial_x \left( \frac{v_y^2}{2} + p \right) = 0$$

integrate from the center,  
where  $v_y = 0$  and  $p = p_m$  to the  
outside where  $v_y = v_{out}$  and  $p = p_0$

$$\frac{v_{out}^2}{2} = p_m - p_0$$

together with eq. from previous slide

$$\frac{B_0^2}{2} = p_m - p_0$$

# Sweet Parker: a scaling for the reconnection rate

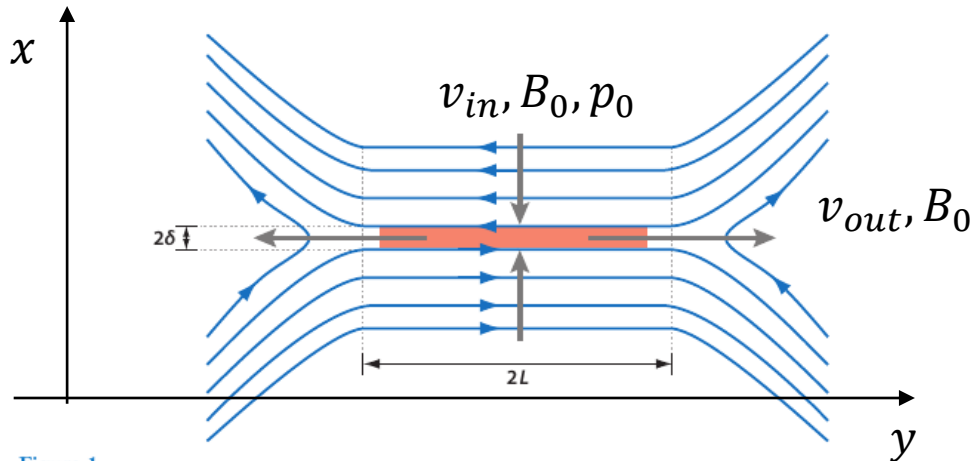


Figure 1

Sketch of magnetic field geometry in Sweet-Parker reconnection. Oppositely directed magnetic fields are brought together over a length  $2L$  and reconnect in a diffusion layer of width  $2\delta$ .

$$\frac{\delta}{L} = \frac{v_{in}}{v_{out}} = \frac{\eta}{\delta v_{out}}$$

$$\frac{\delta^2}{L^3} = \frac{\eta}{L^2 v_{out}}$$

$$\frac{\delta^2}{L^3} = \frac{1}{\tau_R v_{out}}$$

together with

$$\frac{v_{out}^2}{2} = p_m - p_0$$

implies

$$\frac{B_0^2}{2} = p_m - p_0$$

$v_{out} = B_0 = v_A$   
 the velocity outside can be assumed as the Alfvén velocity  $v_A$ , and so

$$\frac{\delta^2}{L^3} = \frac{1}{\tau_R v_{out}} = \frac{\tau_A}{\tau_R L} \quad S = \frac{\tau_R}{\tau_A}$$

and thus

$$\frac{v_{in}}{v_A} = \frac{\delta}{L} = S^{-\frac{1}{2}}$$

reconnection rate  $\tau^{-1}$  proportional to  $S^{-1/2}$

# optional: the issue of "fast reconnection"

- A long-standing problem in reconnection theory is briefly discussed here, i.e., the fast reconnection rates (proportional to the inverse Alfvén time) observed in astrophysical and laboratory systems like in the solar flares and in the tokamak sawtoothing instability.
- A resistive diffusion process would give too slow reconnection rates,  $\tau^{-1} \propto S^{-1}$
- magnetohydrodynamic (MHD) regime: Sweet and Parker<sup>1</sup> consider a two-dimensional current sheet and an incompressible inflow of plasma in the reconnection region gives a faster rate  $\tau^{-1} \propto S^{-0.5}$
- Later, the occurrence of instabilities of the current sheet itself<sup>2</sup>, discovering the possibility of reconnection rates independent of resistive effects  $\tau^{-1} \propto S^0$
- It was also shown that collisionless effects<sup>3</sup> could speed-up the reconnection rate to values compatible with observations
- Boozer<sup>4</sup> claims that the most overlooked feature in modeling fast magnetic reconnection is three-dimensionality.

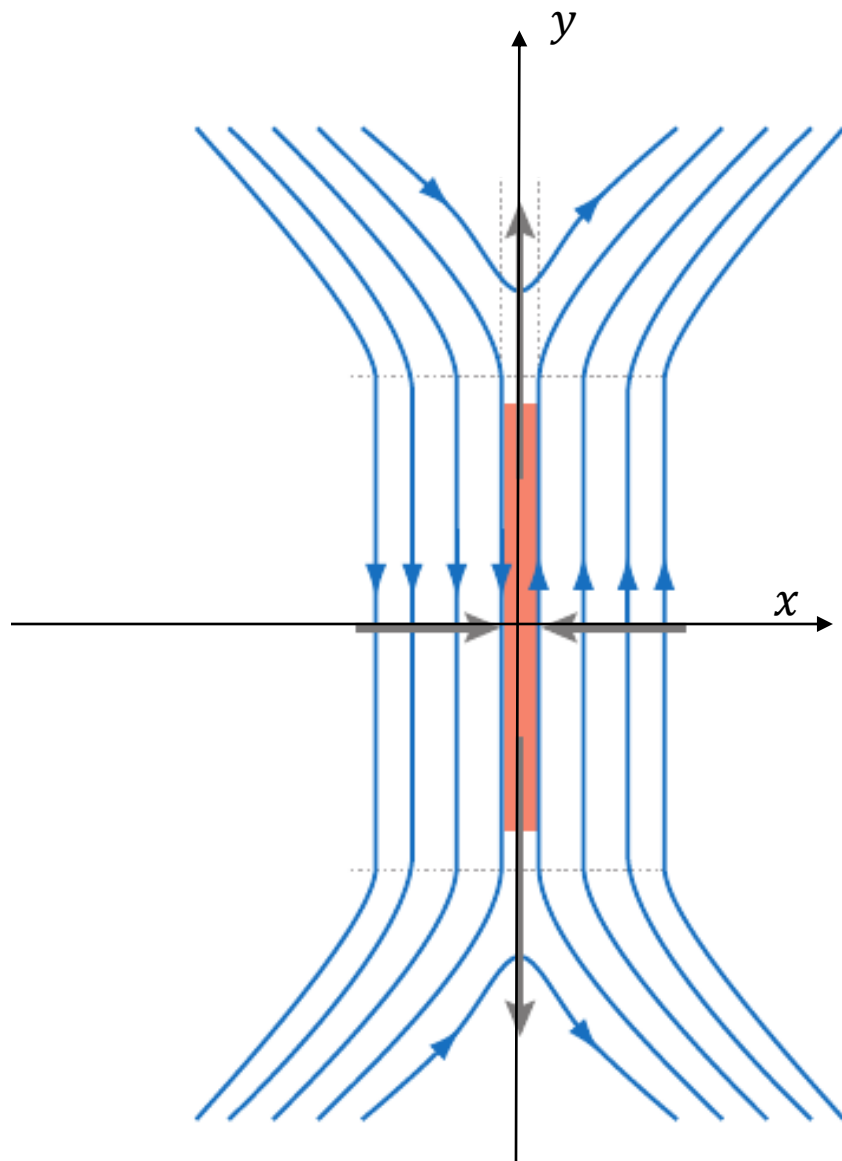
<sup>1</sup> Parker EN (1957) Sweet's mechanism for merging magnetic fields in conducting fluids. *J Geophys Res (1896–1977)* 62(4):509–520.

<sup>2</sup> Bhattacharjee A, Huang YM, Yang H, Rogers B (2009) Fast reconnection in high-Lundquist-number plasmas due to the plasmoid instability. *Phys Plasmas* 16(11):112102

<sup>3</sup> Biskamp D, Schwarz E, Drake JF (1995) Ion-controlled collisionless magnetic reconnection. *Phys Rev Lett* 75:3850–3853.

<sup>4</sup> Boozer AH (2018) Why fast magnetic reconnection is so prevalent. *J Plasma Phys* 84(1):715840102.

# magnetic islands: naive.



- aim of the instability: reconnect the magnetic field in the  $x \sim 0$  region;
- a small perturbation in the  $\hat{x}$  direction arises, active in the resistive layer.

- For simplicity we write it like this:

$$B_x \sim B_{x0}(x) e^{\textcolor{red}{y}t} \sin(\textcolor{teal}{k}y)$$

- for small perturbations the magnetic field in the  $\hat{y}$  direction can be approximated by

$$B_y \sim B'_{y0} x$$

# magnetic islands: naive.

$$B_x \sim B_{x0} e^{\gamma t} \sin(ky)$$

$$B_y \sim B'_{y0} x$$

- compute magnetic field lines ( $\mathbf{B} \times d\mathbf{l} = 0$ ):

$$\frac{dx}{dl} = B_x \quad , \quad \frac{dy}{dl} = B_y$$

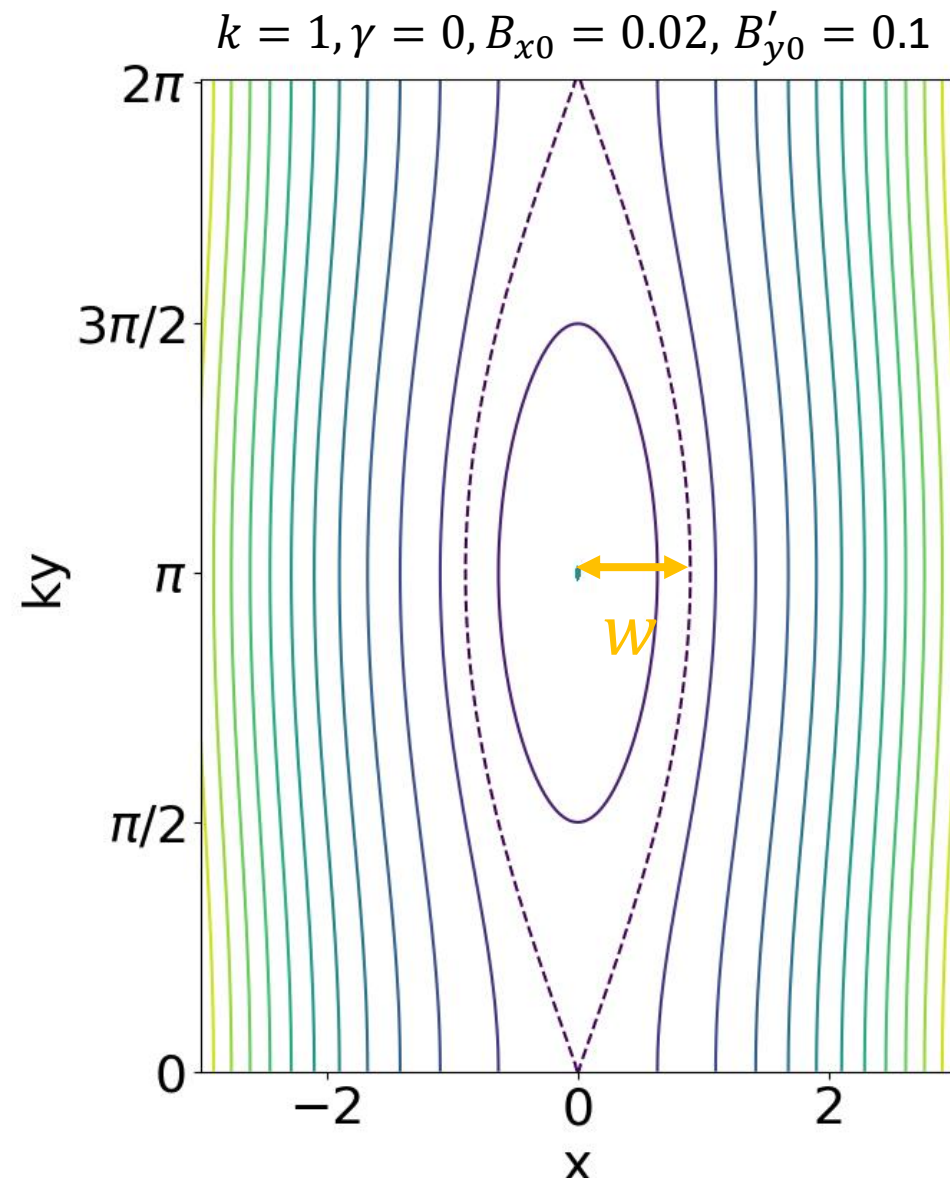
- and thus:

$$\frac{dx}{dy} = \frac{B_x}{B_y} = \frac{B_{x0}}{B'_{y0} x} e^{\gamma t} \sin(ky)$$

- integration gets you:

$$B'_{y0} \frac{x^2}{2} + B_{x0} e^{\gamma t} \frac{\cos(ky)}{k} = cost$$

# magnetic islands: half width $w$



$$B_x \sim B_{x0} e^{\gamma t} \sin(ky)$$

$$B_y \sim B'_{y0} x$$

$$B'_{y0} \frac{x^2}{2} + B_{x0} e^{\gamma t} \frac{\cos(ky)}{k} = c_0$$

- dashed separatrix @ $x = 0, y = 0$ :

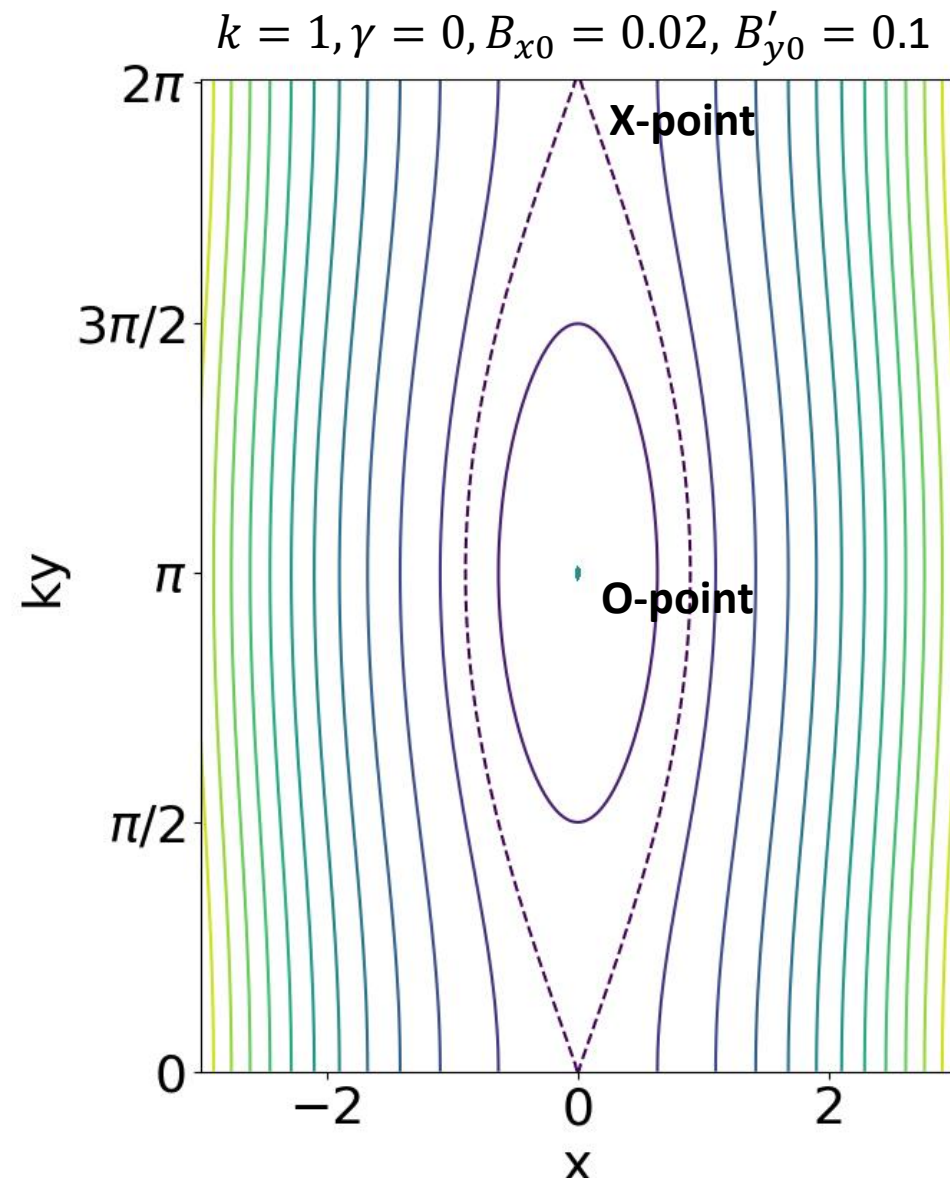
$$c_0 = B_{x0} \frac{e^{\gamma t}}{k}$$

- follow the contour level until  $ky = \pi$ :

$$x^2 = \frac{2c_0}{B'_{y0}} \rightarrow x = \sqrt{\frac{2B_{x0} e^{\gamma t}}{B'_{y0} k}}$$

i.e.  $w \propto \sqrt{B_{x0}}$

# magnetic islands: half width $w$



$$B_x \sim B_{x0} e^{\gamma t} \sin(ky)$$

$$B_y \sim B'_{y0} x$$

$$B'_{y0} \frac{x^2}{2} + B_{x0} e^{\gamma t} \frac{\cos(ky)}{k} = c_0$$

- dashed separatrix @ $x = 0, y = 0$ :

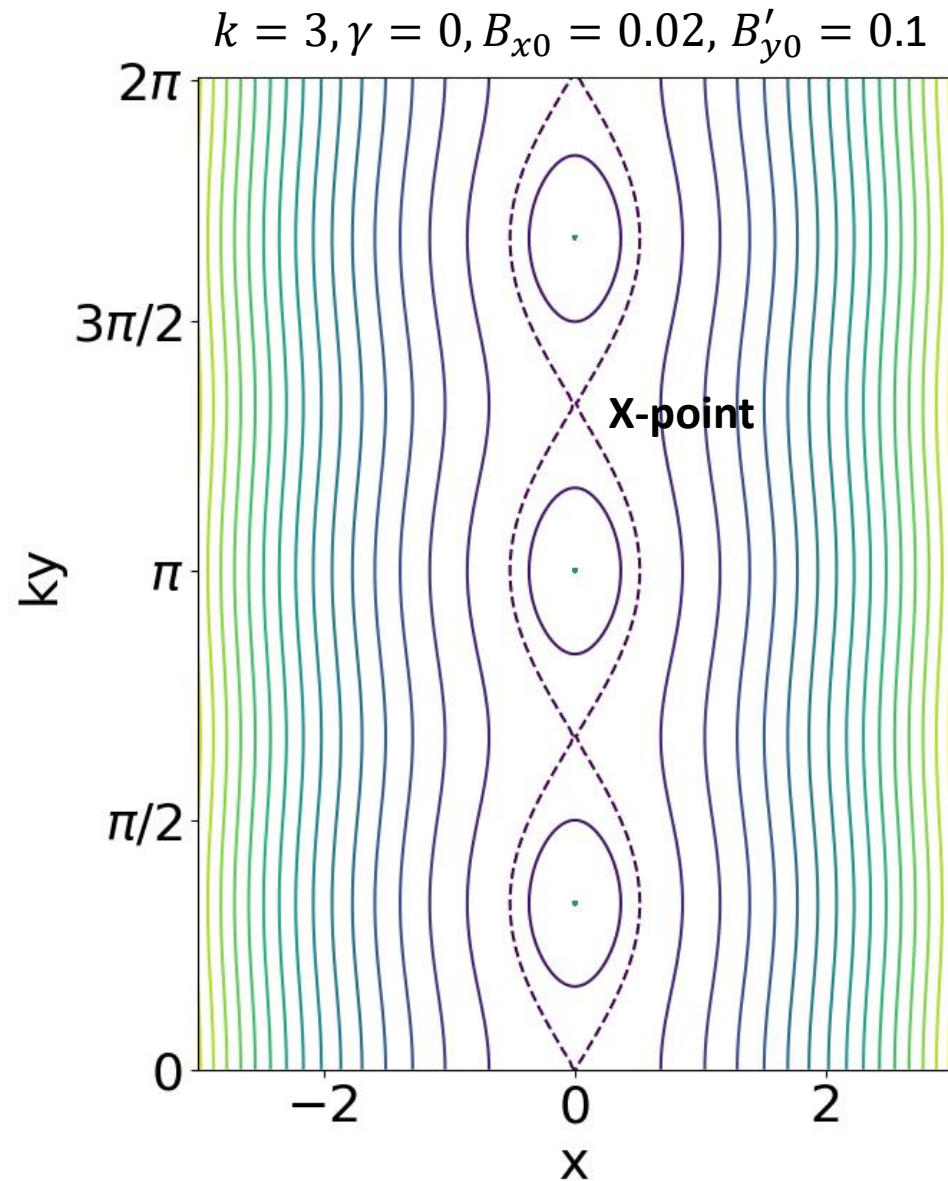
$$c_0 = B_{x0} \frac{e^{\gamma t}}{k}$$

- follow the contour level until  $ky = \pi$ :

$$x^2 = \frac{2c_0}{B'_{y0}} \rightarrow x = \sqrt{\frac{2B_{x0} e^{\gamma t}}{B'_{y0} k}}$$

i.e.  $w \propto \sqrt{B_{x0}}$

# magnetic islands



$$B_x \sim B_{x0} e^{\gamma t} \sin(ky)$$

$$B_y \sim B'_{y0} x$$

$$B'_{y0} \frac{x^2}{2} + B_{x0} e^{\gamma t} \frac{\cos(ky)}{k} = c_0$$

- dashed separatrix @ $x = 0, y = 0$ :

$$c_0 = B_{x0} \frac{e^{\gamma t}}{k}$$

- follow the contour level until  $ky = \pi$ :

$$x^2 = \frac{2c_0}{B'_{y0}} \rightarrow x = \sqrt{\frac{2B_{x0} e^{\gamma t}}{B'_{y0} k}}$$

i.e.  $w \propto \sqrt{B_{x0}}$

# magnetic islands: where magnetic reconnection can happen in a tokamak

- If we Fourier decompose every perturbation in a "cylindrical tokamak" (always in the spirit of keeping things simple) we can categorize them using two wave numbers for the two periodic coordinates  $\theta$  and  $z$ , i.e.  $\mathbf{k} = (m, n)$ , i.e. a generic perturbation is of the form  $B_{pert} \sim e^{\gamma t} e^{m\theta + \frac{nz}{R}}$  with  $R$  representing the axial height of the cylinder and the aspect ratio of the rectified torus.
- the condition for instability is the so-called resonance condition  $\mathbf{k} \cdot \mathbf{B} = 0$
- In pinches this happens locally when the safety factor has a rational value, i.e. magnetic field lines close on themselves after a certain number of turns in toroidal and poloidal direction. Because of the shear of the magnetic field, if we follow the field lines on both sides of the resonant surface with  $q = q_r = 2$  (we choose a particular case) they will either lag behind or advance the field line on the resonant surface, creating a component of the magnetic field relative to the  $q = q_r$  surface which changes sign across it. A transversal magnetic field, manifesting itself as a current-driven "tearing" instability results in the opening of a magnetic island, as observed looking at the helical flux function contour levels.
- Clearly, infinitely many rational numbers can be 'fitted in' between  $q(0)$  and  $q(a)$ . However, another rule, found by more refined analysis, is that only large wavelengths tend to be unstable to resistive-tearing modes.

# nonlinear evolution / saturation

- In practice, nonlinear effects will limit the growth of magnetic islands when significant modifications are produced in the underlying magnetic configuration on which our stability analysis was based.
- Such effects begin to appear as soon as the island width becomes comparable to the width of the resistive layer, as was shown in a paper (P.H. Rutherford 1973 Phys. Fluids **16** 1903).
- When the island grows to a significant fraction of the size of the overall configuration, it can affect the gross current profile tending to stabilize the tearing mode.

# nonlinear evolution: Rutherford equation

- a basic equation: Faraday in radial direction
- integrate along the island width  $w$  (and consider  $B_r$  approximately constant in the island)
- remind that  $w^2 \propto B_r$
- define the "linear stability index"  $\Delta' = \frac{1}{B_r} \partial_r B_r|_{r_s-w/2}^{r_s+w/2}$

(this index depends only on the ideal MHD of the system)

Instability occurs when  $\Delta'$  exceeds a critical value,  
 $\Delta' > \Delta_c \geq 0$

$$\partial_t B_r = \frac{\eta}{\mu_0} \frac{\partial^2 B_r}{\partial r^2}$$

$$w \partial_t B_r = \frac{\eta}{\mu_0} \partial_r B_r \Big|_{r_s-w/2}^{r_s+w/2}$$

$$w \partial_t w^2 = \sim \frac{\eta}{\mu_0} \partial_r B_r \Big|_{r_s-w/2}^{r_s+w/2}$$

$$\partial_t w = \frac{\eta}{2\mu_0} \frac{1}{B_r} \partial_r B_r \Big|_{r_s-w/2}^{r_s+w/2}$$

$$\partial_t w \sim \frac{\eta}{\mu_0} \Delta'(w)$$

# nonlinear evolution: Rutherford equation

- but, for sufficient island width the previous linear estimates of  $\Delta'$  are no more correct, in fact tearing modes can affect the underlying equilibrium parameters in two ways:
  - i) flattening of the current density gradient
  - ii) flattening of temperature profiles.
- thus, the minimal estimate is (without proof) that

$$\Delta'(w) = \Delta'(0) \left( 1 - \frac{w}{w_{sat}} \right)$$

$$\partial_t w \sim \frac{\eta}{\mu_0} \Delta'(w)$$

- giving a solution of Rutherford equation

$$w(t) = w_{sat} \left( 1 - e^{-t \frac{r^2 \Delta'(0)}{\tau_R w_{sat}}} \right)$$

# nonlinear evolution: Rutherford equation

- further effects: plasma finite pressure, toroidicity (and thus non-inductive currents like:
  - bootstrap current due to the pressure gradient of trapped particles;
  - Pfirsch-Schlüter current that guarantees  $\nabla \cdot \mathbf{J} = 0$  even on the torus

$$\frac{\tau_R}{r_{\text{res}}} \frac{dW}{dt} = r_{\text{res}} \Delta'(W) + c_{\text{sat}} \frac{r_{\text{res}}^{3/2}}{R_0^{1/2}} \frac{L_q}{L_p} f_{GGJ} \beta_p \frac{1}{W} \quad *$$

- increases the possibility for tearing modes instability (neoclassical tearing modes) with increased plasma pressure

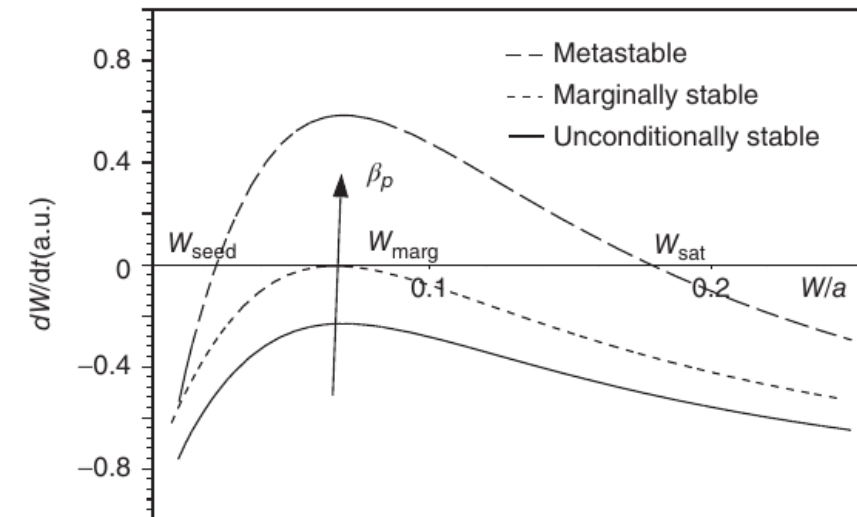


**Figure 12.2** Schematic stability diagram for NTMs, indicating the existence of unconditional stability (no stationary point), marginal stability (one stationary point), and

metastability (two stationary points of which only  $W_{\text{sat}}$  is stable). For simplicity, only  $W_0$  has been included as small island term for this plot.

\*remind the definition of "decay length", for example  $L_p = -\frac{n}{\frac{dp}{dr}} = \frac{-1}{d\ln(p(r))}$

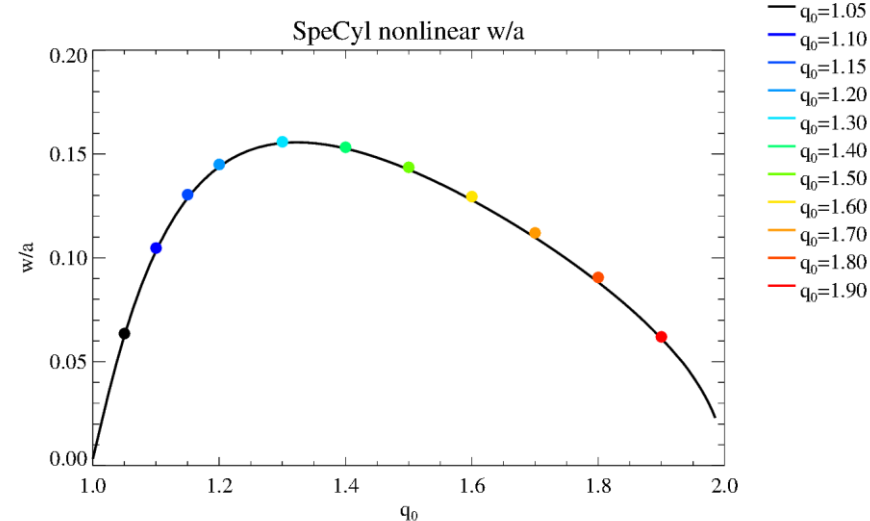
# nonlinear evolution: more advanced models

The saturation of the tearing mode is a difficult issue, and its solution has been a stepwise process covering almost three decades, starting from 1977 [a],

Many effects involved: plasma finite pressure, toroidicity (and thus non-inductive currents like Pfirsch-Pfirsch-Schlüter current that guarantees  $\nabla \cdot \mathbf{J} = 0$  even on the torus and others) .

A rigorous solution to the simple tearing mode problem in cylindrical geometry is given in [b]:

$$\frac{\mu_0}{\eta_{eq}(r_s)} \frac{dw}{dt} = 1.22\nabla' + w \left\{ \frac{A^2}{2} \ln \frac{w}{w_0} - 2.21A^2 + 0.4 \frac{A}{r_s} + \frac{B}{2} + 0.17\lambda \frac{A^2 s}{2-s} \right\} + o(w)$$



comparison between the saturation width given by analytical formula (60) and 3D nonlinear MHD computations, varying on axis safety factor  $q(0)$ .

[a] R. B. White, D. A. Monticello, and M. N. Rosenbluth, Phys. Fluids 20, 800 (1977).

[b] Arcis, Escande, Ottaviani, Rigorous approach to the nonlinear saturation of the tearing mode in cylindrical and slab geometry, Physics of Plasma 13, 052305 (2006)

# magnetic islands: numerical solution

- numerically solved with main approximations:
  - zero-pressure;
  - constant and stationary density;
- for this purpose we use the SpeCyl MHD-code, (IPP, Consorzio RFX [a])
- using  $\eta = 10^{-6}$ ,  $\nu = 10^{-3}$

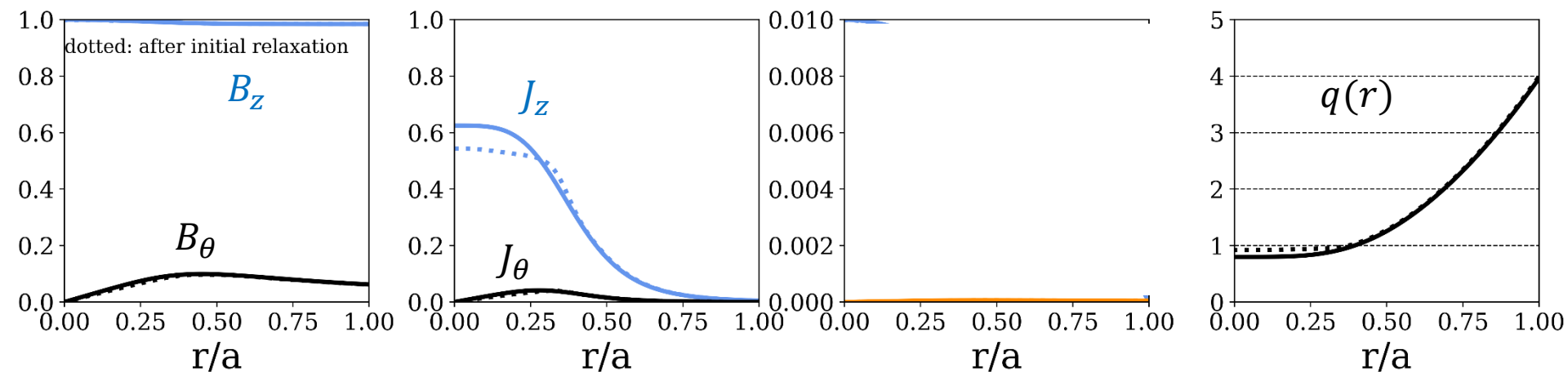
$$\frac{\partial \boldsymbol{v}}{\partial t} + \boldsymbol{v} \cdot \nabla \boldsymbol{v} = \boldsymbol{J} \times \boldsymbol{B} + \nu \nabla^2 \boldsymbol{v}$$

$$\boldsymbol{E} + \boldsymbol{v} \times \boldsymbol{B} = \eta \boldsymbol{J}$$

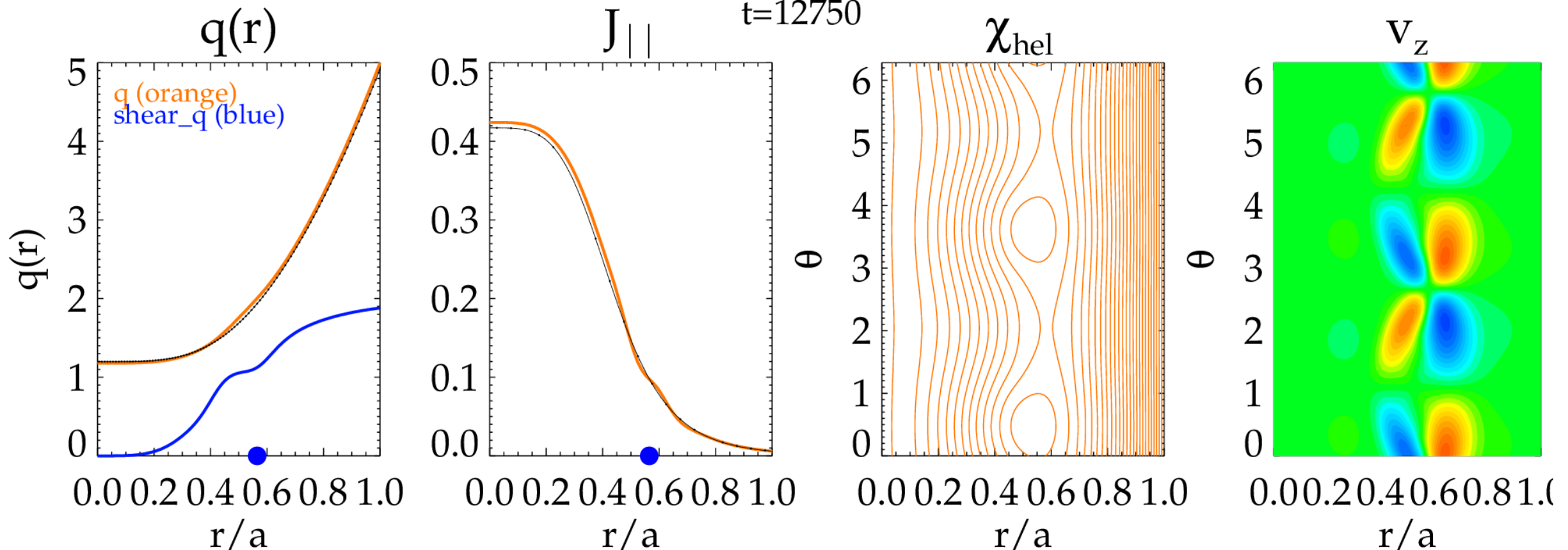
$$\nabla \times \boldsymbol{E} = -\frac{\partial \boldsymbol{B}}{\partial t}$$

$$\nabla \times \boldsymbol{B} = \boldsymbol{J}$$

$$\nabla \cdot \boldsymbol{B} = 0$$



# video: nonlinear evolution of a tearing mode with m=2 n=-1



remind: safety factor in cylindrical geometry  $q(r) = \frac{rB_z(r)}{RB_\theta(r)}$

$$\text{magnetic shear } s = \frac{rd(\ln q)}{dr}$$

# nonlinear evolution: effect on kinetic profiles

- Electron heat transport in constant-density, zero flow magnetized plasmas is:

$$\partial_t T + \nabla \cdot \mathbf{q} = S = \eta J^2 \quad (1)$$

- the heat flux  $\mathbf{q}$  is given by:  $\mathbf{q}[T] = -\chi_{\perp}(T)\nabla_{\perp}T + \mathbf{q}_{\parallel}[T]$

$$\partial_t T - \frac{\chi_{\parallel}}{\chi_{\perp}} \partial_s^2 T = \nabla_{\perp}^2 T + S$$

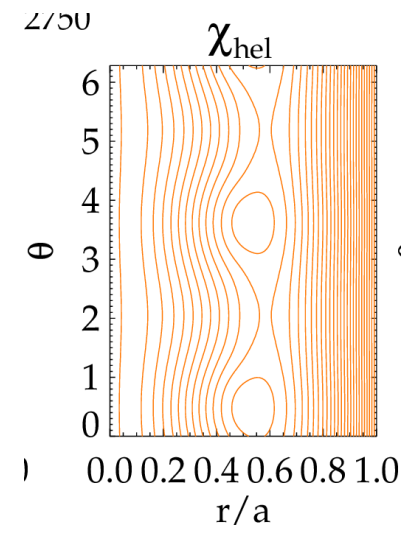
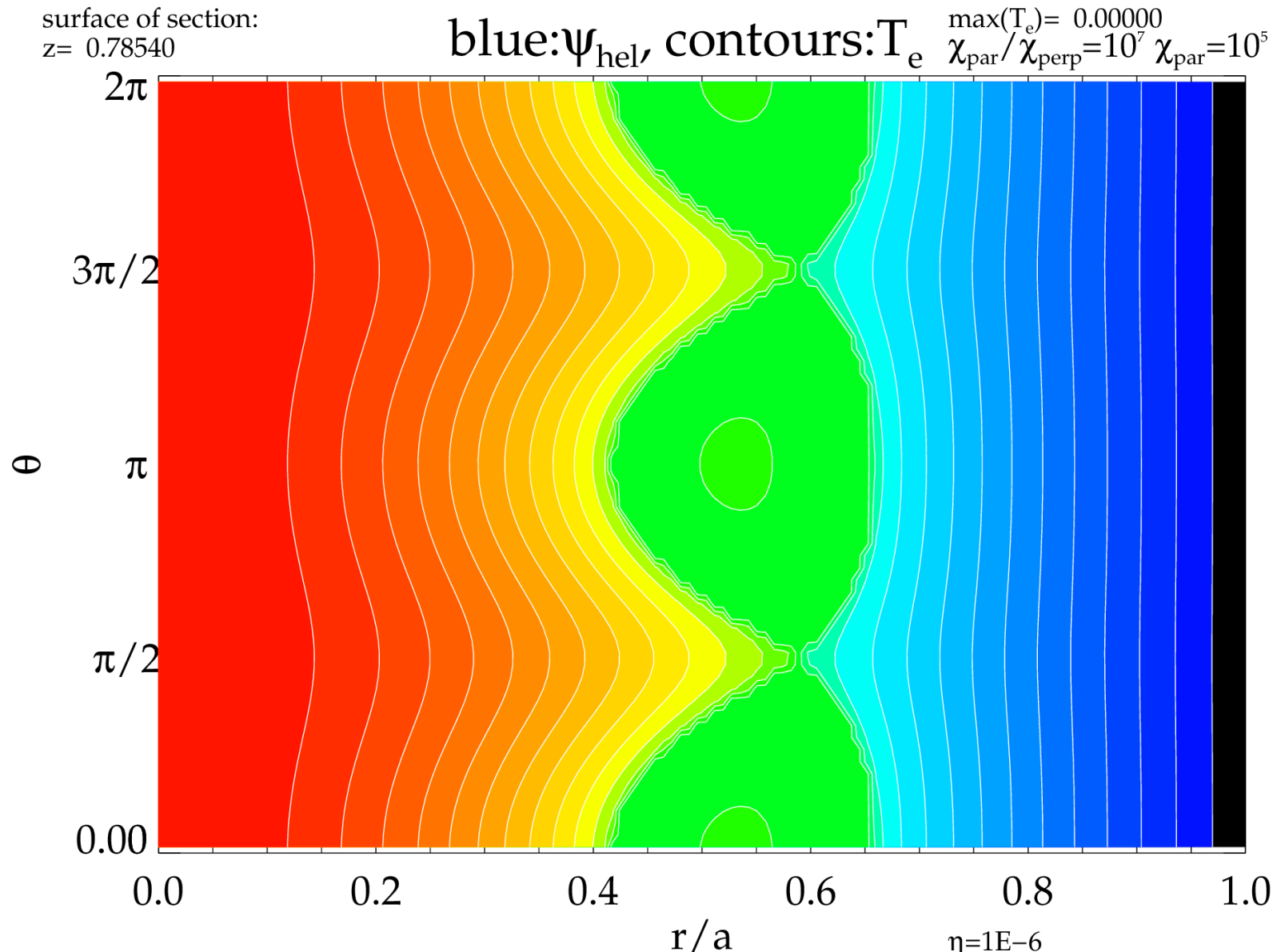
$$\epsilon = \frac{\chi_{\perp}}{\chi_{\parallel}} \approx 10^{-8:-10}$$

high anisotropy ratio in hot magnetized plasmas.  
 We consider uniform and constant diffusion coefficient

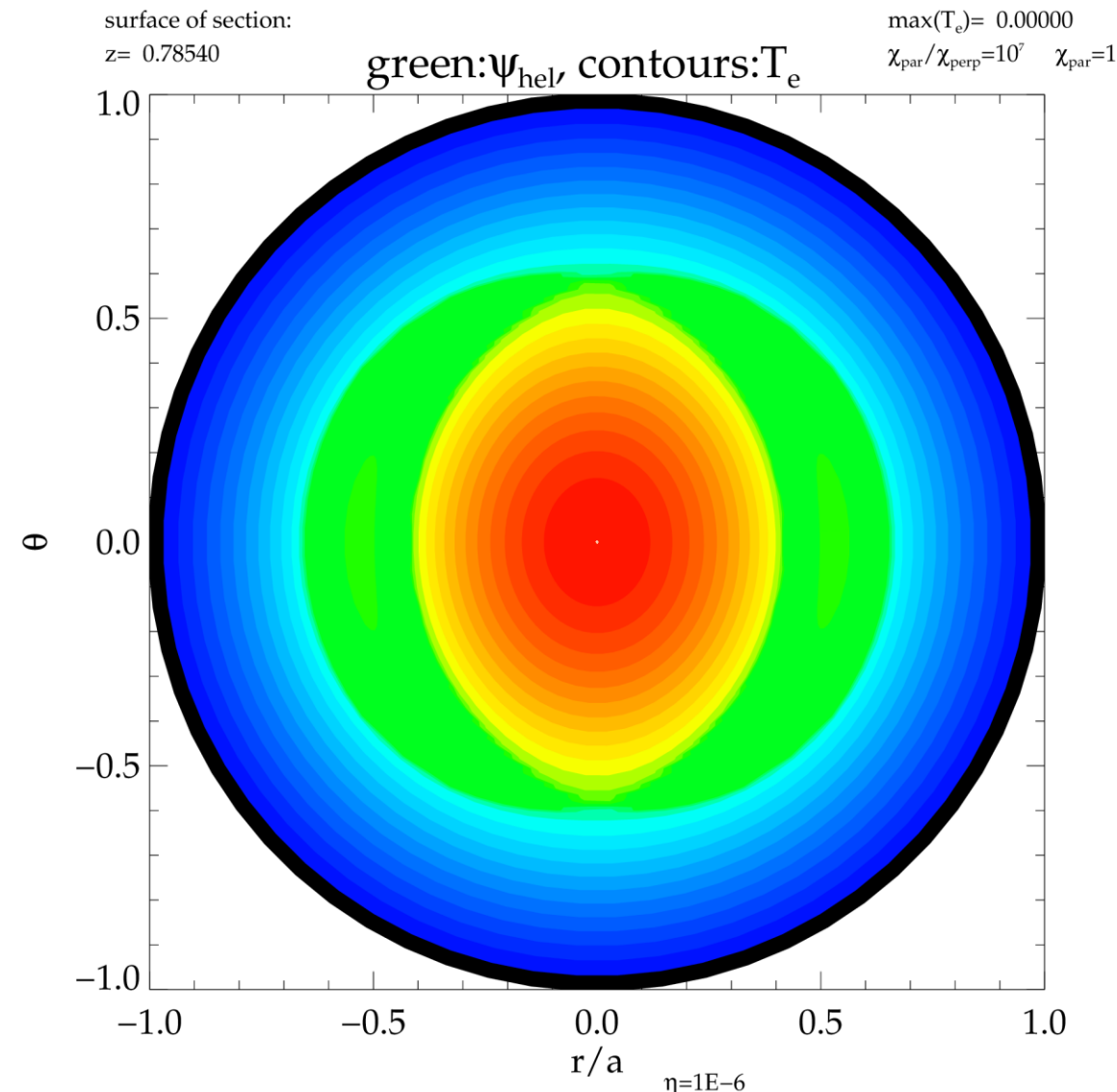
- Lagrangian approach, follow magnetic field lines wandering
- We solve equation (1) with the T3D code [a]

[a] L. Chacón, D. del-Castillo-Negrete, C.D. Hauck **JCP** 272 (2014)

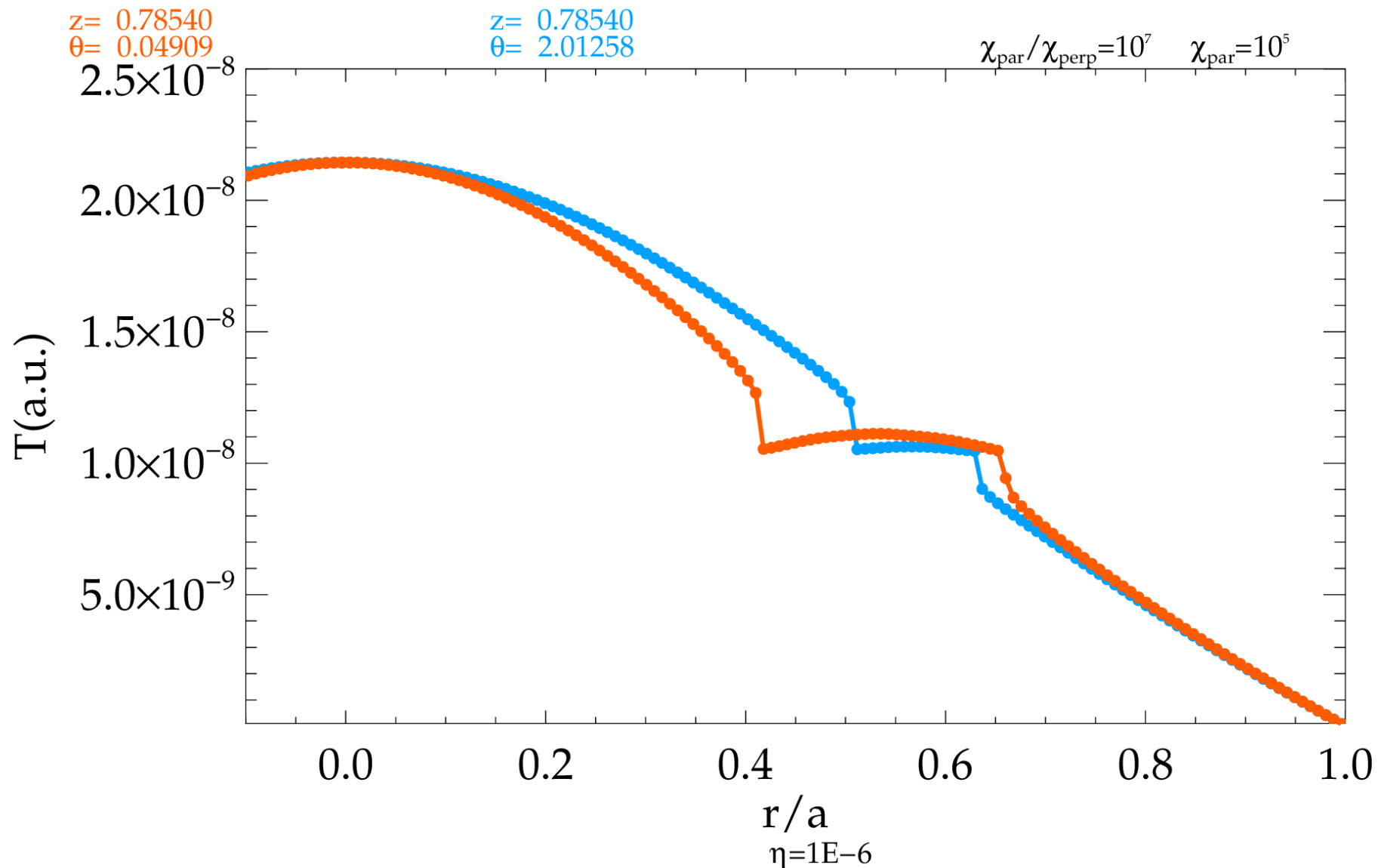
# nonlinear evolution: effect on kinetic profiles



# nonlinear evolution: effect on kinetic profiles



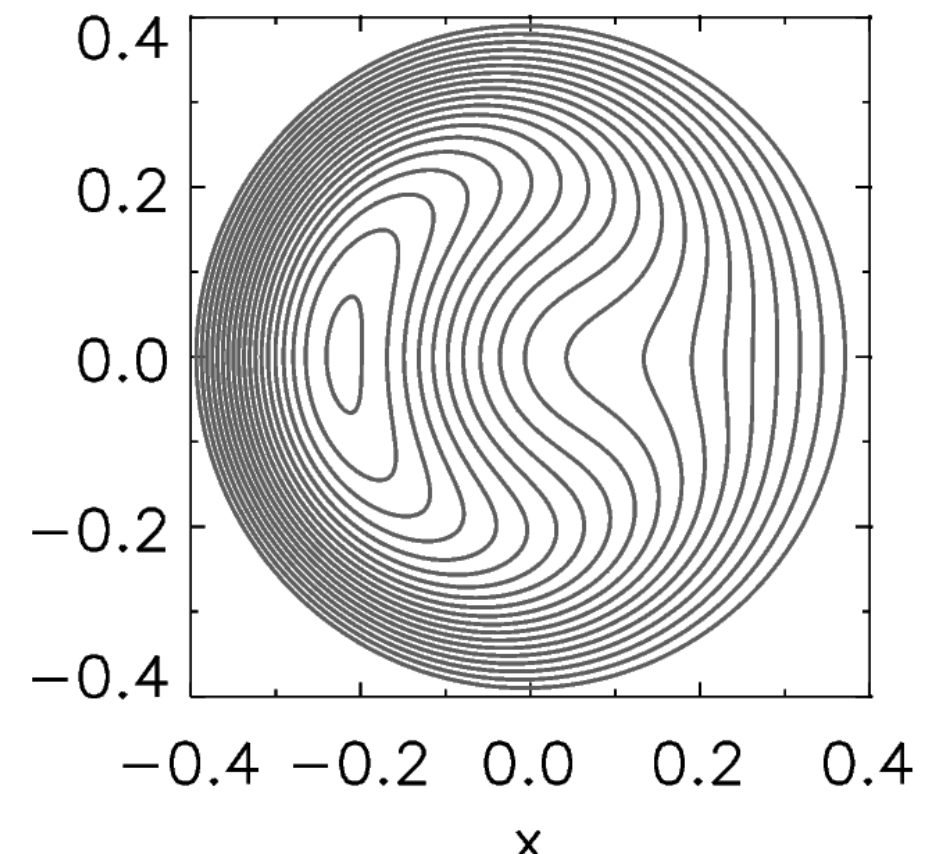
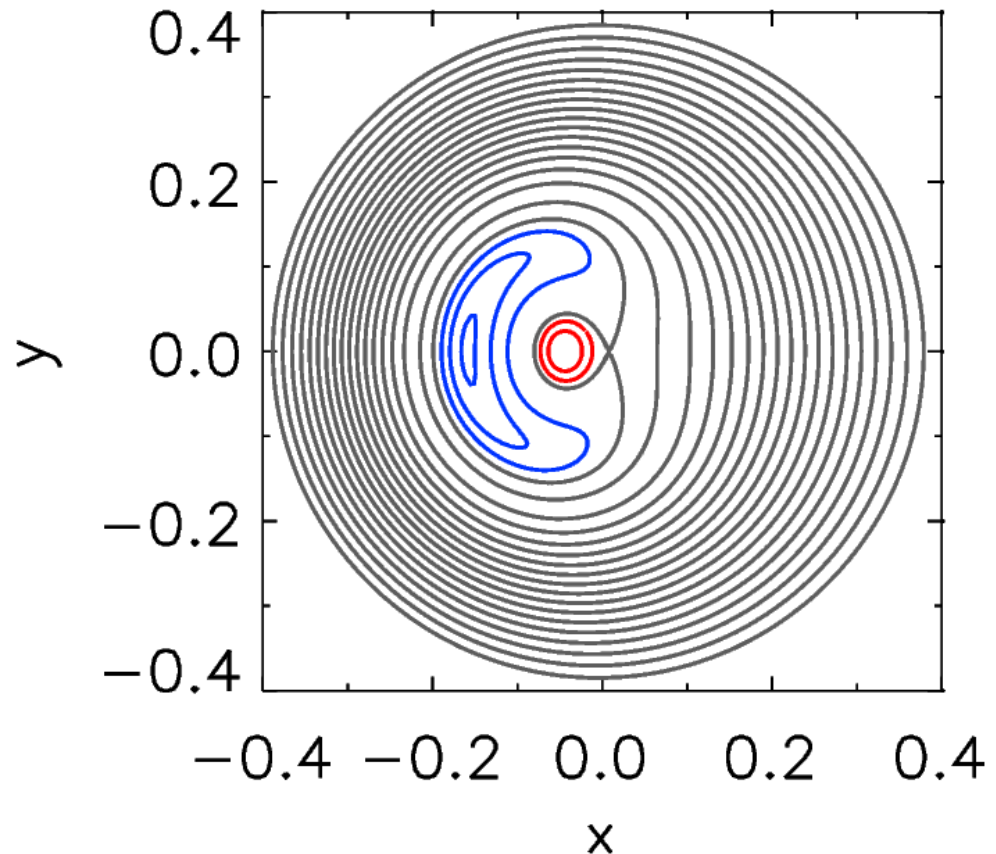
# nonlinear evolution: effect on kinetic profiles



# when plasma current is 10x higher than in tokamaks: reversed-field pinches

the magnetic island becomes so unstable that in the end it completely change the topology of the magnetic field and the original red axisymmetric red axis is destroyed and the new axis of the magnetic field is given by the O-point of the island (blue).

More on Thursday afternoon, RFP theory, S. Cappello.





pause

The sawtooth instability

i.e. effect of the «special» 1,1 mode

Subtle: non-ideal effects; nonlinear cycles;

Fishbone instability: 1,1+energetic particles

## Remind: linear theory of internal kink modes

- One of the basic tokamak instabilities: found by analytically solving the energy equation imposing  $\xi_a = 0$  and using a step-function for  $\xi(r)$ . Expansion of energy equation to fourth order → subtle (finite resistivity, two fluids effect, finite Larmor radius can change stability)

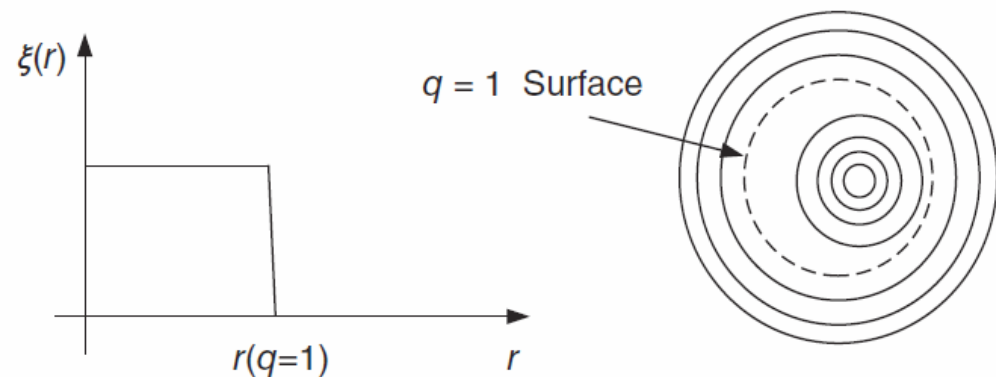


**Figure 4.5** Test function used to minimize  $\delta W$  for internal kink analysis.

Necessary condition not to have an internal kink mode:  $q(0) > 1$

$$q(r) = \frac{rB_z}{RB_\theta}$$

$$\int dr B_\theta = \mu_0 I_P \rightarrow \frac{2B_\theta}{r} = \mu_0 J(r)$$

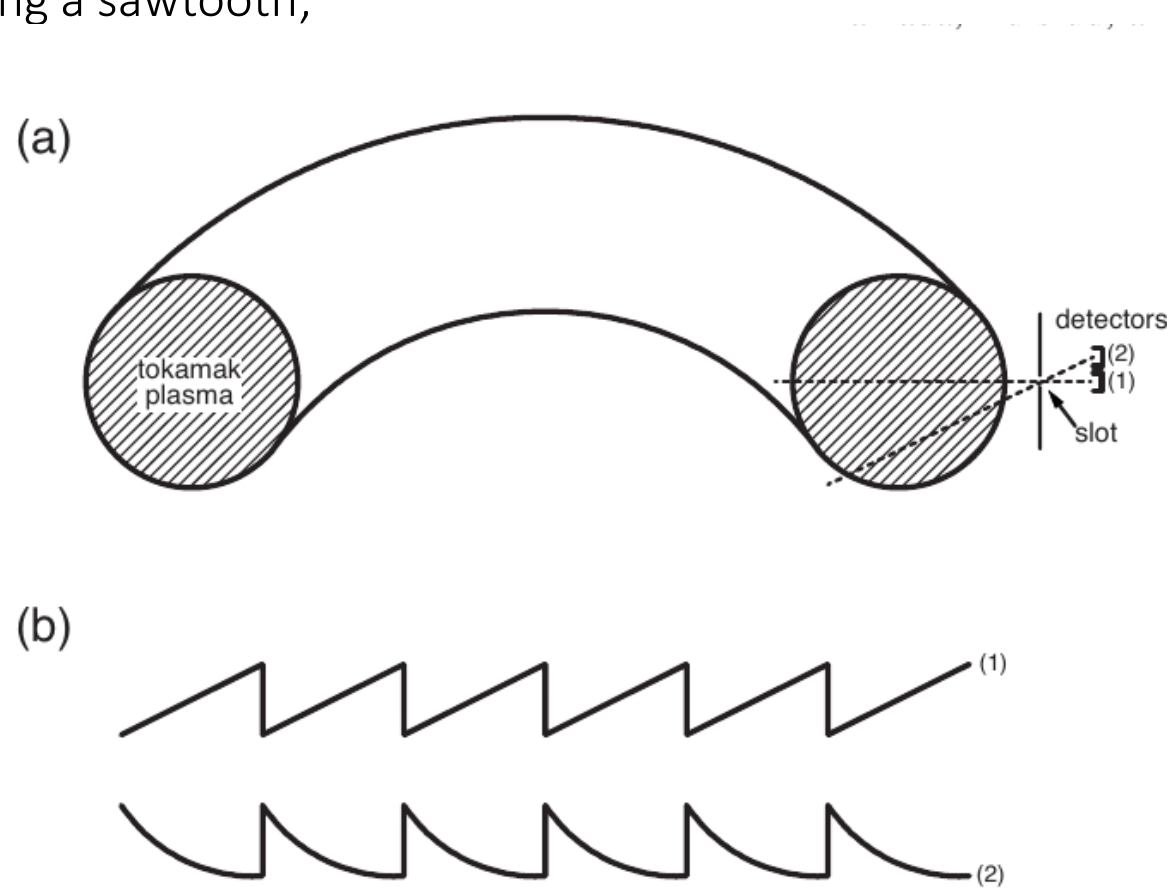
$$\rightarrow \text{around } r \sim 0 : q(0) = \frac{2B_z(0)}{R\mu_0 J(0)}$$

$$q(0) > 1 \rightarrow J(0) < \frac{2B_z}{\mu_0 R}$$

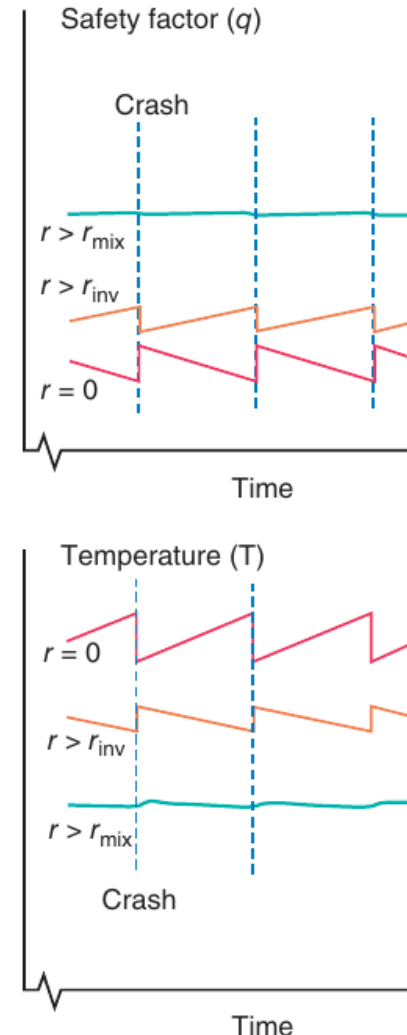
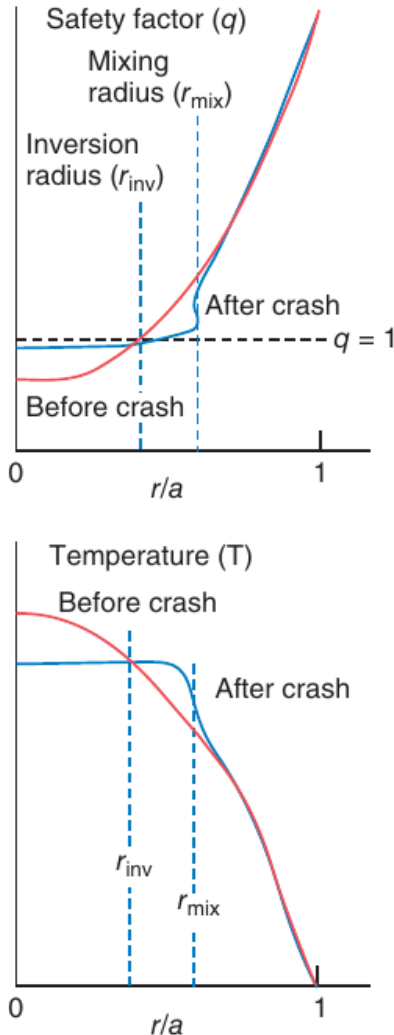
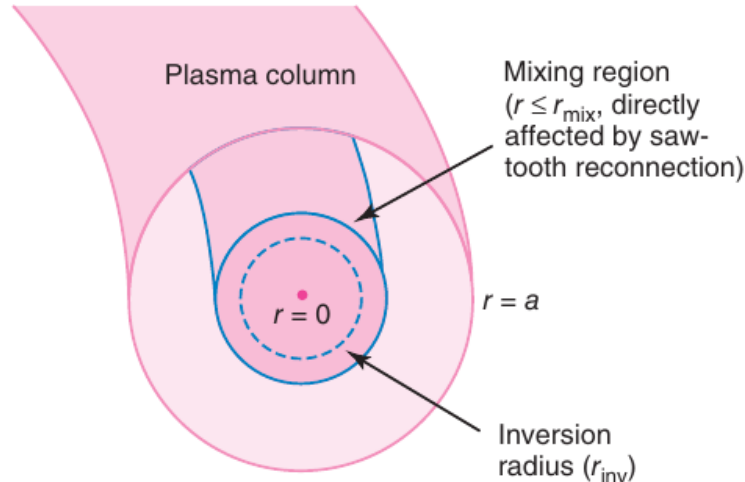
Limit on maximum  $I_P$ , i.e. limit on confinement time.

# internal kink modes: nonlinearity

- The sawtooth instability is observed in most conventional tokamak scenarios at reasonably high current, that is when a  $q = 1$  surface is present in the plasma;
- a periodic modulation of the central temperature and density is seen, with a time trace resembling a sawtooth;



# internal kink modes: nonlinearity

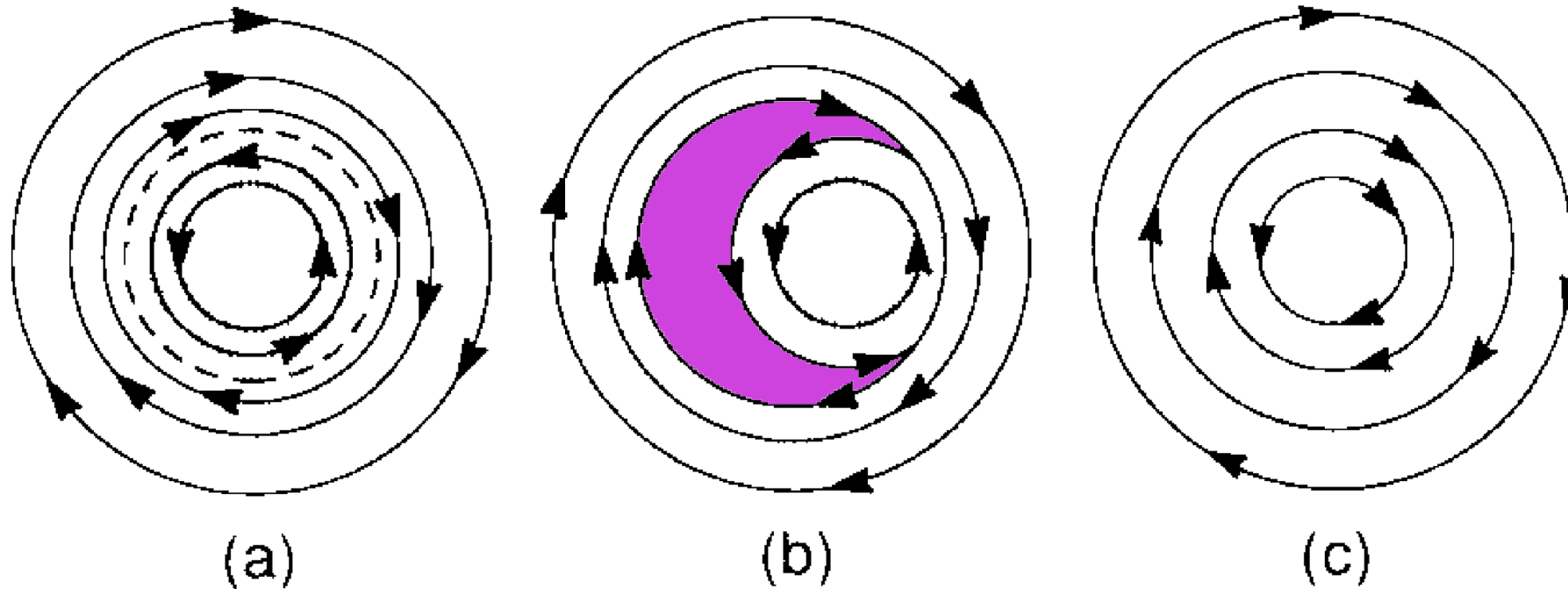


from Zohm,  
Magnetohydrodynamic  
Stability of Tokamaks  
Wiley (2015)

# some physics

- Good energy confinement in the core  $\rightarrow T_e$  increases;
- Resistivity decreases ( $\eta \propto T_e^{-3/2}$ )
- Ohmic heat deposition increases ( $P_\Omega \propto \eta J^2 \sim \frac{E_0^2}{\eta}$ ), with  $E_0$  toroidal electric field and  $E_0 \sim \eta J$
- Electron temperature further increase and thus also plasma current
- this implies that  $J$  is further peaked
- A peaked current profile means that  $q_0$  decreases (below 1), the **1,1 mode becomes unstable**, it mixes the plasma inside the resonance radius redistributing its energy outside.
- redistribution of heat, particles, and poloidal flux
- instability plays an important role in determining the quasi-stationary (i.e. sawtooth-cycle averaged) parameters of tokamak discharges. In particular, it limits the peaking of temperature, density, and current density profiles.

# Resistive internal kink: reconnection and island formation



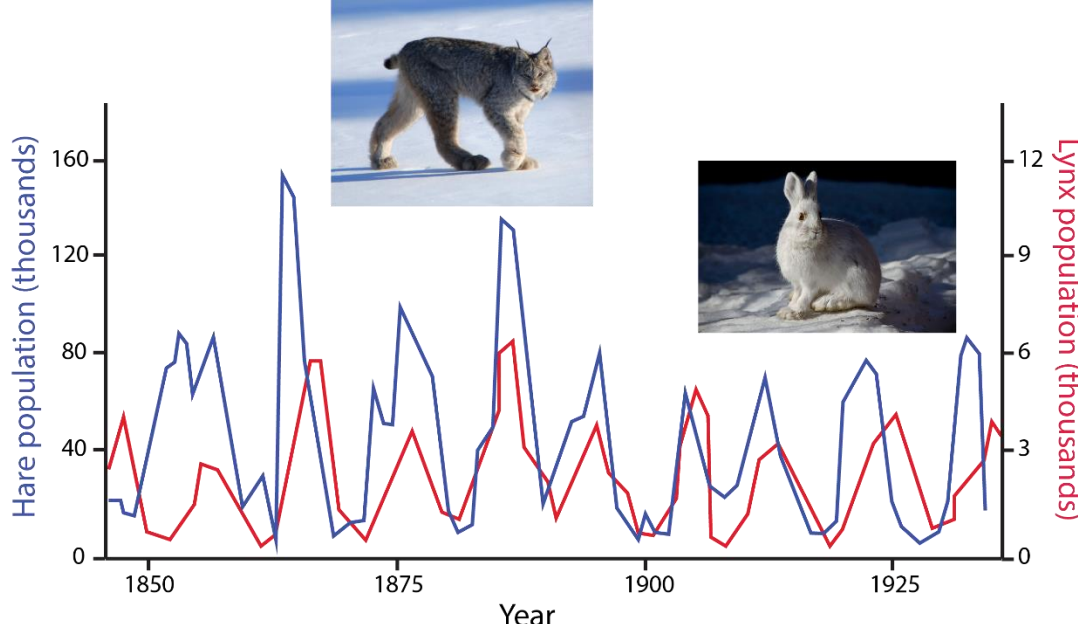
# effects of nonlinearity: nonlinear cycles and stochasticity

Non-linear cycles can arise from a system in which the **driving force** is continuously supplied and an **instability** that acts to remove the drive is triggered above a certain threshold.

Such a system can have different stationary solutions: one possibility is a state in which all time derivatives vanish and an equilibrium value is reached where the system just sits at marginal stability.

Another, more interesting case is the possibility of limit cycles: these are a periodic growth of an instability which removes the driving force such that it needs some time to be restored.

Basic example:  
Lotke-Volterra  
equations for  
predator-prey  
systems.  
not possible  
linearly

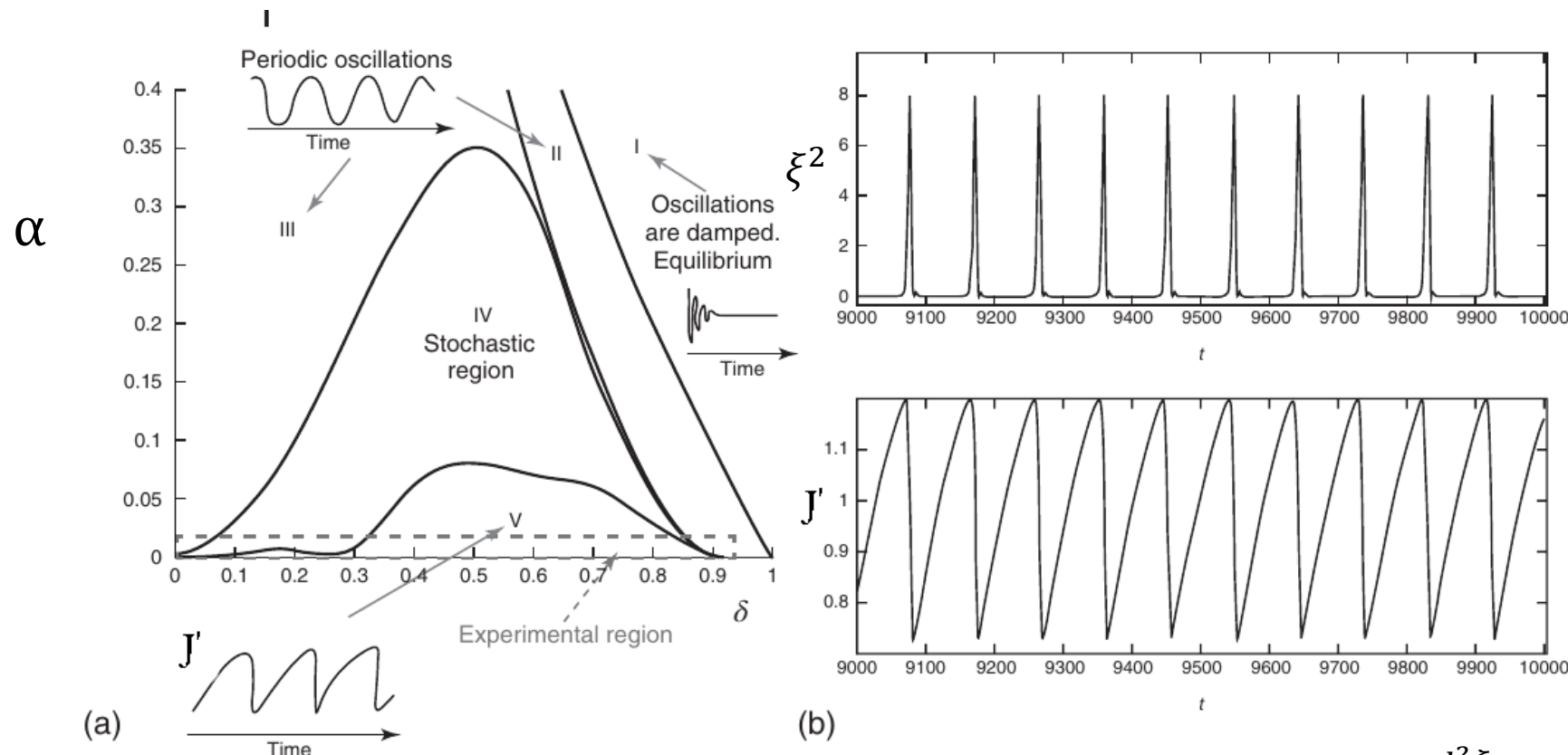


$$\frac{dx}{dt} = ax + \beta xy$$
$$\frac{dy}{dt} = \gamma y - \beta xy$$

# a simple nonlinear model to describe sawtoothing

- limit cycles can be obtained from a set of two non-linearly coupled differential equations representing the temporal evolution of the instability drive and the MHD mode (amplitude  $\xi$ ).
- In our case: the drive is the current density gradient  $J'$
- $\frac{d^2\xi}{dt^2} = (J' - 1)\xi - \delta \frac{d\xi}{dt}$  : equation for temporal evolution of MHD instability.  $\delta$  is a normalized damping.
- We need an equation for the temporal evolution of the drive:
- $\frac{dJ'}{dt} = \alpha(P - J' - \beta \xi^2 J')$
- the first two terms on the rhs represents a balance between power  $P$  increasing  $J'$  and  $J'$  itself, plus the **nonlinear term** providing the coupling between the two equations.
- $\alpha$  represents the ratio between transport timescale (which tends to resolve high  $J'$ ) and timescale related to the growth of MHD mode.

# some solutions of the micro-model



$$\frac{d^2\xi}{dt^2} = (J' - 1)\xi - \delta \frac{d\xi}{dt}$$

From H. Zohm, 2015, Magnetohydrodynamics stability of tokamaks, Wiley-VCH.  
 From D. Constantinescu et al (2011) A low-dimensional model system for quasi-periodic plasma perturbations. Phys. Plasmas, 18, 062307

$$\frac{dJ'}{dt} = \alpha(P - J' - \beta \xi^2 J')$$

- if no coupling, i.e.  $\beta = 0$ , temporal evolution moves towards a stationary state:  $J'(t) = P - e^{-\alpha t}$
- If no damping mechanism of instability is present, i.e.  $\delta = 0$ , harmonic oscillator if  $J' < 1$ , exponential growth if  $J' > 1$
- If high damping is present, oscillations are damped → equilibrium
- If  $\alpha \rightarrow 0$ , a regime of nonlinear oscillations can be found. Short MHD time scales compared to transport can evolve in a sawtooth way.

$$\frac{d^2\xi}{dt^2} = (J' - 1)\xi - \delta \frac{d\xi}{dt}$$

$$\frac{dJ'}{dt} = \alpha(P - J' - \beta \xi^2 J')$$

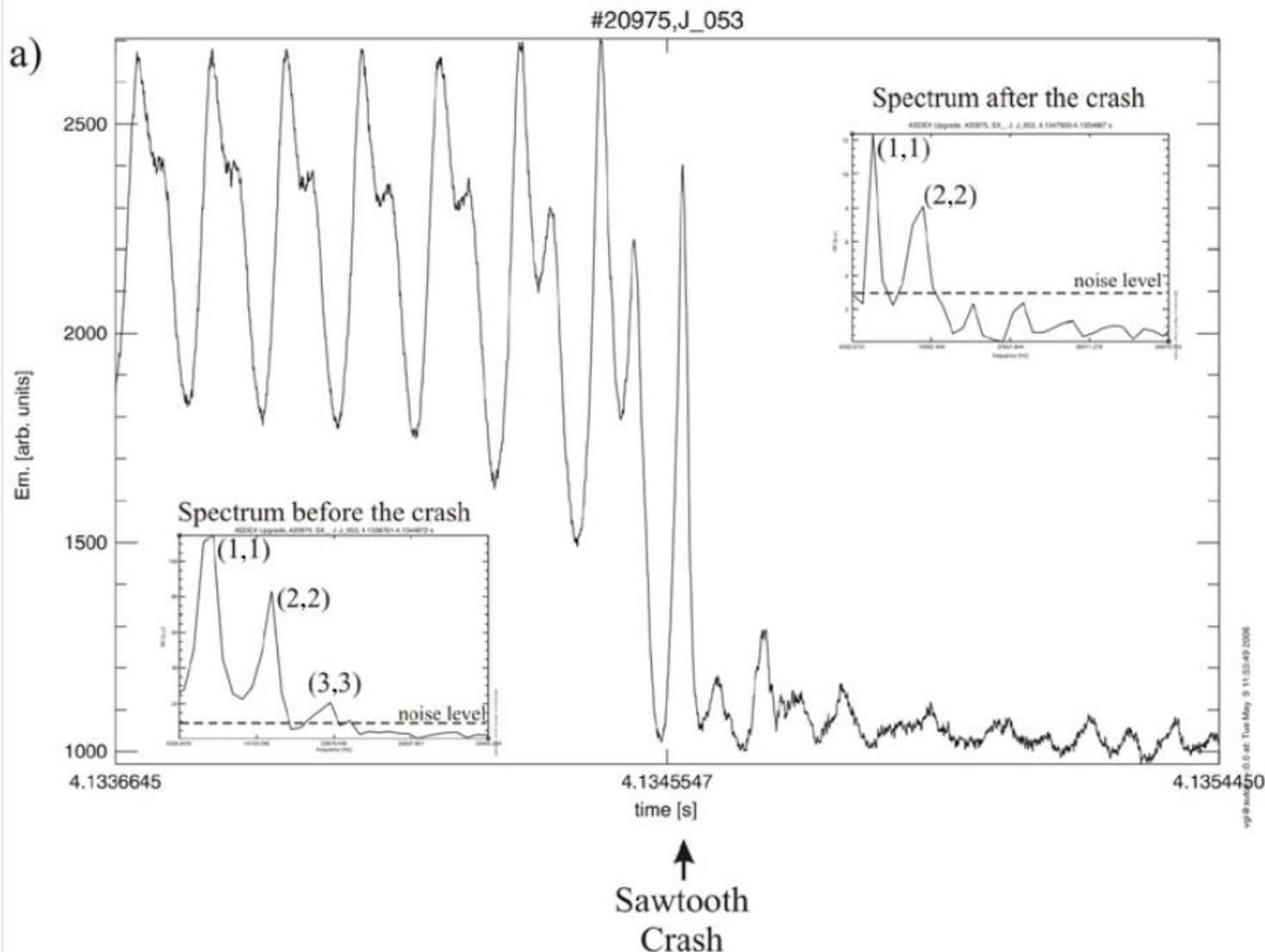
- very simplified: more advanced criteria to measure the steepness of the current gradient rely on the so-called "normalized magnetic shear at the  $q = 1$  surface", the normalized shear being defined as

$$s(r) = r \frac{d \ln q(r)}{dr} = \frac{r}{q} \frac{dq(r)}{dr}.$$

- Instability sets in only over a threshold in  $s(r|_{q(r)=1})$  [a]

[a] Porcelli, Boucher, Rosenbluth PPCF 38, 2163 (1998)

# Nonlinearity in (1,1) mode before sawtooth crash



From Iguchine et al Nucl. Fusion **47** (2007) 23–32

# Stochasticization during sawtooth crash

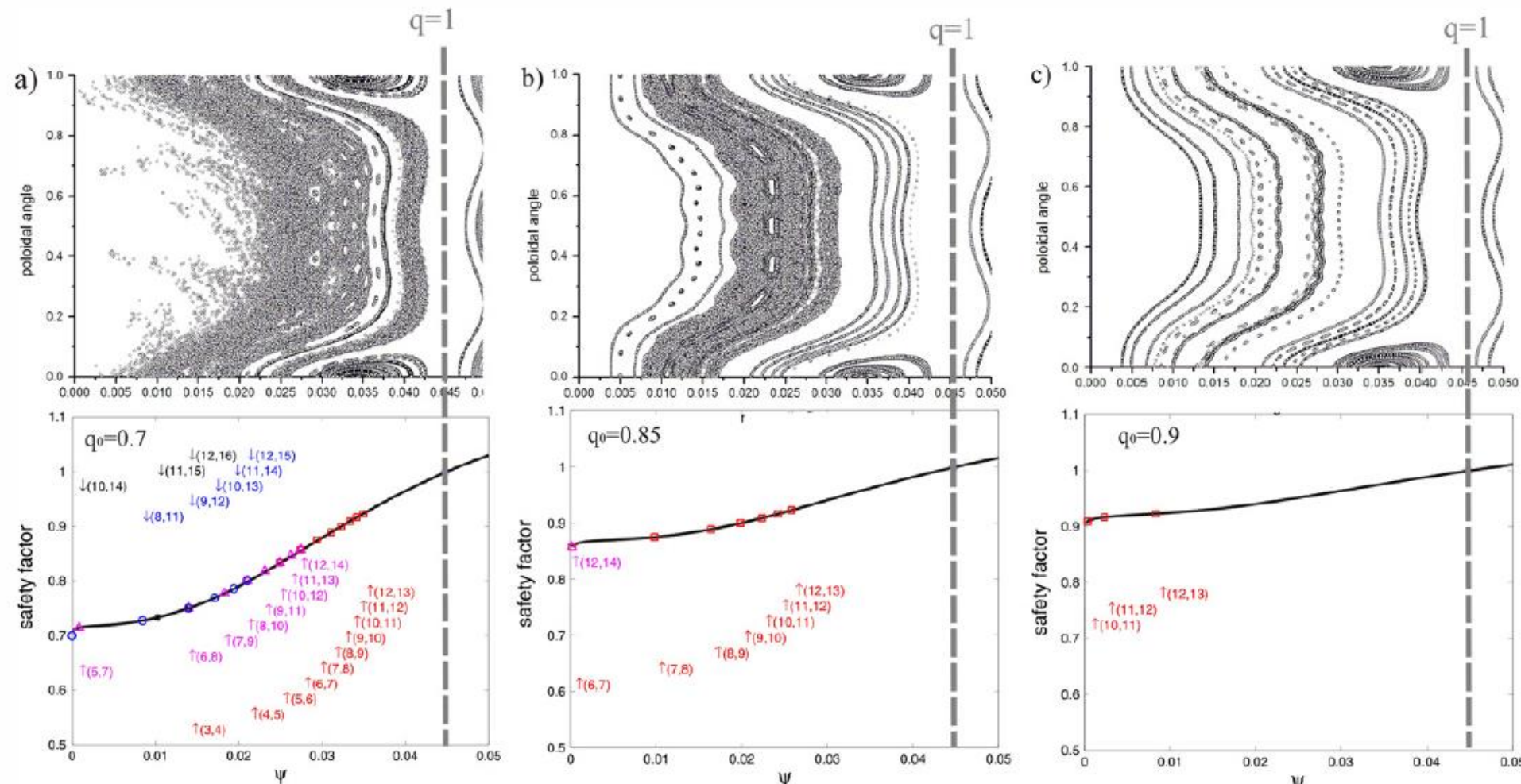


**Figure 9.** Poincaré plots for the same perturbations  $(1, 1) + (2, 2) + (3, 3)$  as in figure 4 but for different safety factor profiles. Note that stochasticization strongly depends on the existence of the low-order rational surfaces which are marked on the safety factor curves.

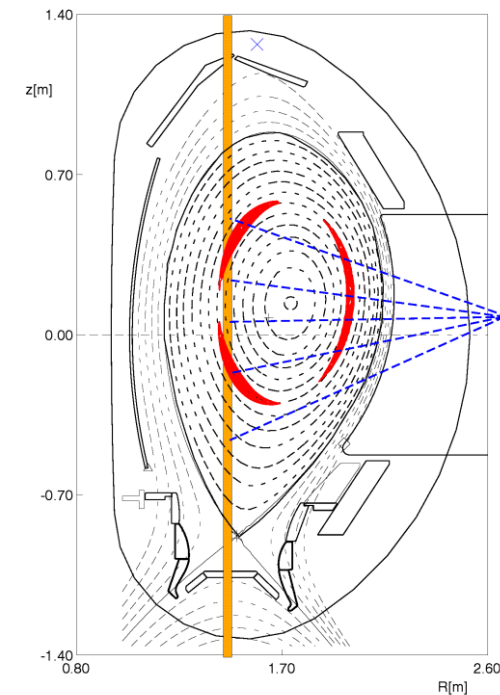
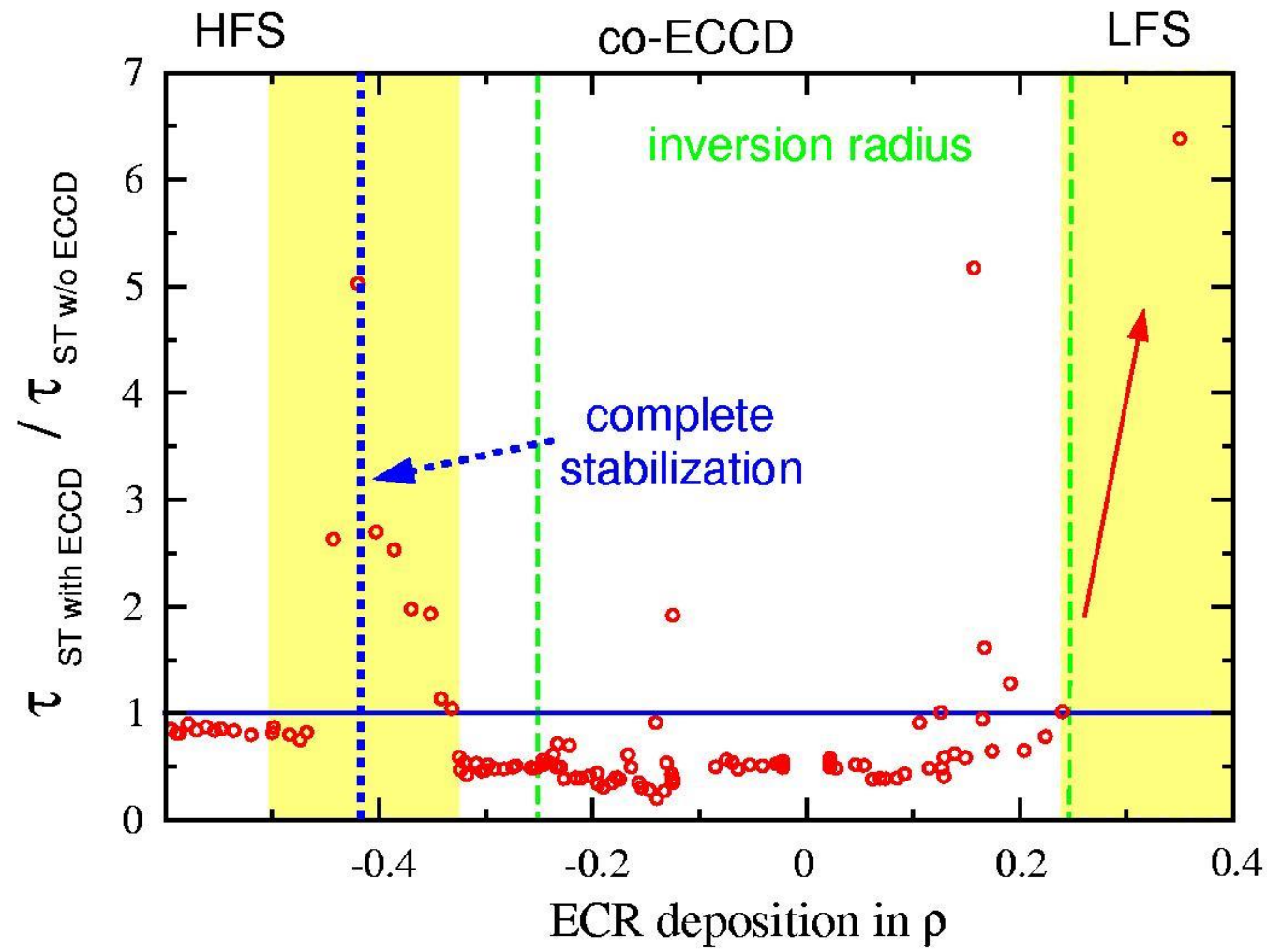
(a) Central  $q$ -value is 0.7; (b) central  $q$ -value is 0.85; (c) central  $q$ -value is 0.9

From Igochine et al Nucl. Fusion **47** (2007) 23–32

# more info about sawtoothing

- roles of sawtoothing: limit the peaking of temperature, density, and current density profiles;
- redistribution of energy and particles from core to edge: NEGATIVE;
- redistribution of impurities and He ashes (from fusion): POSITIVE.
- → need of **active control scheme to tailor** exactly the energy loss & core impurities control
- fast particles have stabilizing effects, alfa particles expected to stabilize.

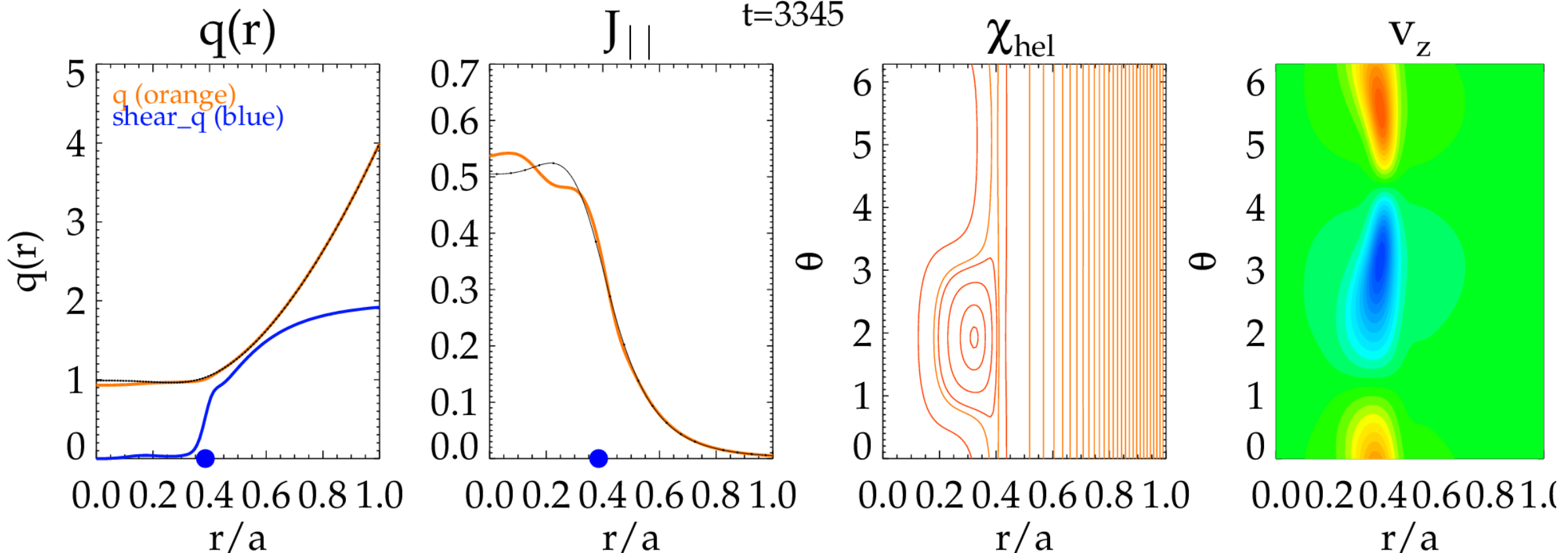
# Sawtooth tailoring by Electron Cyclotron Current Drive



$$\omega_{ECCD} \sim \omega_{ce} = \frac{eB}{m_e}$$

resonant interaction between wave and  $e^-$

# video: nonlinear evolution of a tearing mode with $m=1$ $n=-1$



questions?





pause



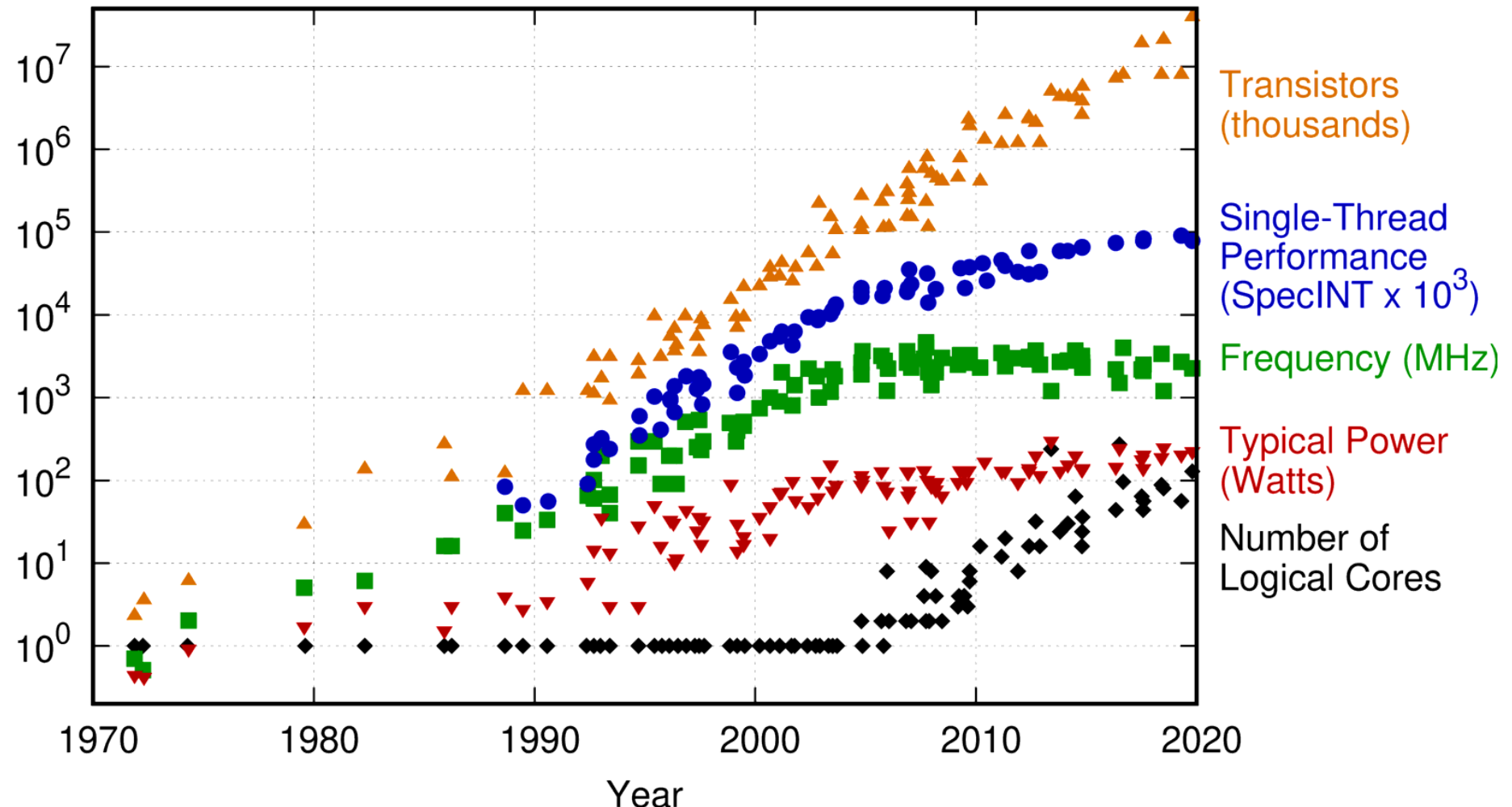
# Evolution drives: technological constraints

- Power wall
- Scaling wall
- Memory wall
- Towards accelerated architectures

- remind:  $P = cV^2f$

with  $P$ : power,  $V$ : voltage,  $f$ : frequency

## 48 Years of Microprocessor Trend Data



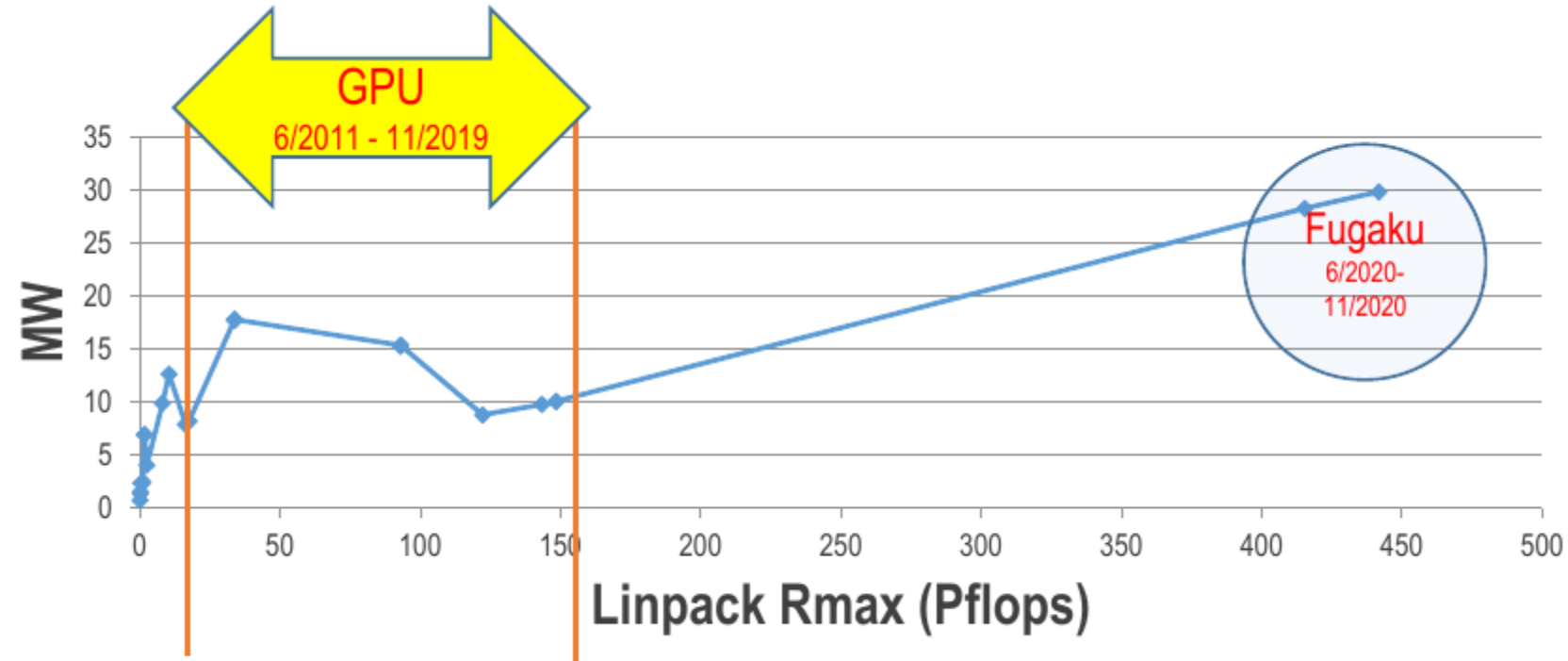
Original data up to the year 2010 collected and plotted by M. Horowitz, F. Labonte, O. Shacham, K. Olukotun, L. Hammond, and C. Batten  
New plot and data collected for 2010-2019 by K. Rupp



# future trends

- Moore's law comes to an end. Probable limit of transistor's size around 3 - 5 nm
- Need to design new structure for transistors
- Limit of circuit size: yield decrease with the increase of surface, chiplets will dominate
- Data movement will be the most expensive operation;
  - One or more accelerator per node
  - Accelerator type will depend on applications
  - GPU (AI)
  - FPGA (Field-Programmable Gate Array)
  - Neuromorphic computing (<https://www.intel.com/content/www/us/en/research/neuromorphic-computing.html>)
  - Quantum accelerator

acceleration is needed to save power



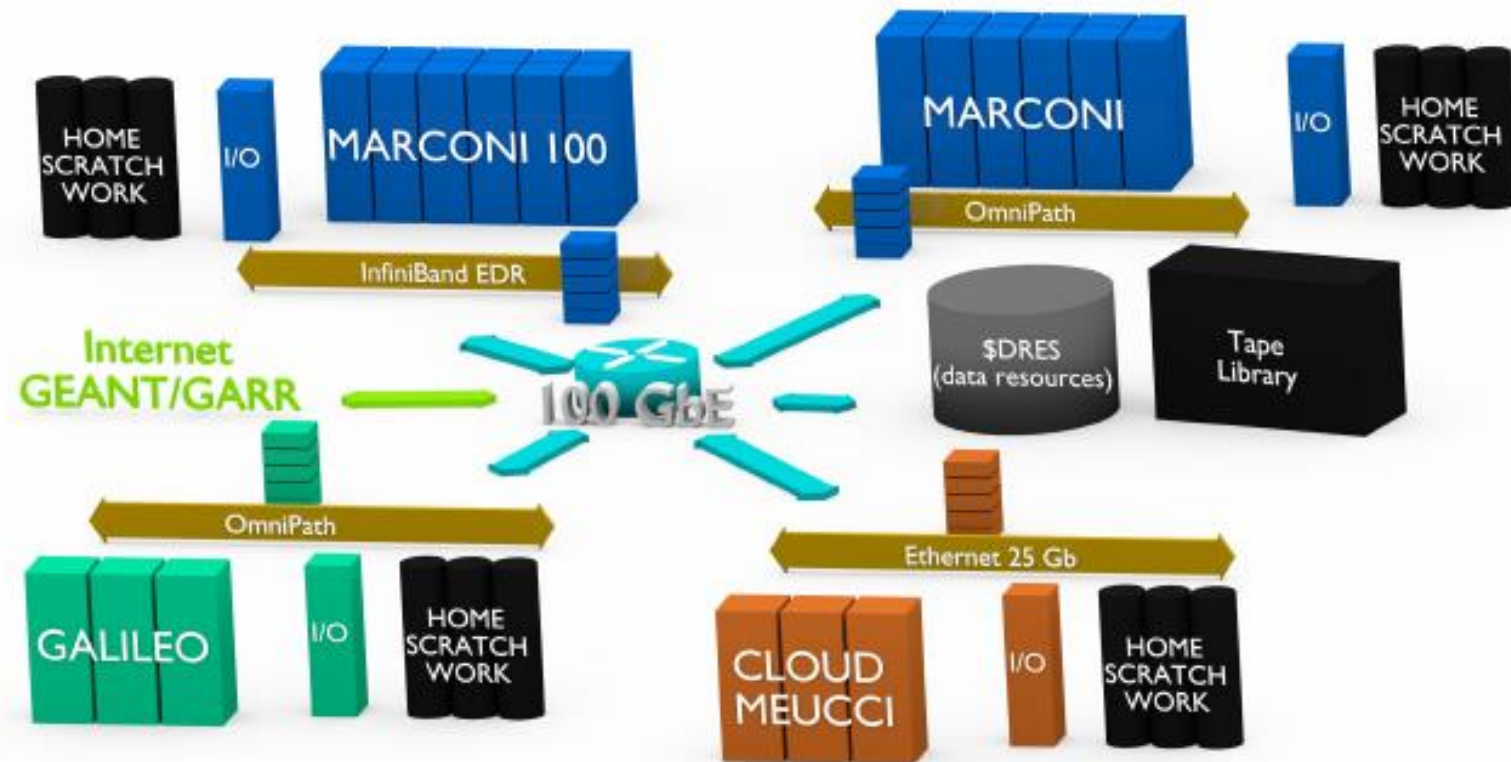
all (pre)Exascale machines to be built in the next few years are accelerated with GPUs

# future trends / 2

- Big trends:
  - C++ is getting momentum → new codes
  - Fortran is losing attraction
- It is high time to program for GPUs
- OpenMP looks like the best bet for the future
  - Especially for Legacy codes and Fortran codes
- C++ might be the best option in the long run

example of a HPC infrastructure

# CINECA Infrastructure



## Marconi100: the Power AC922 model

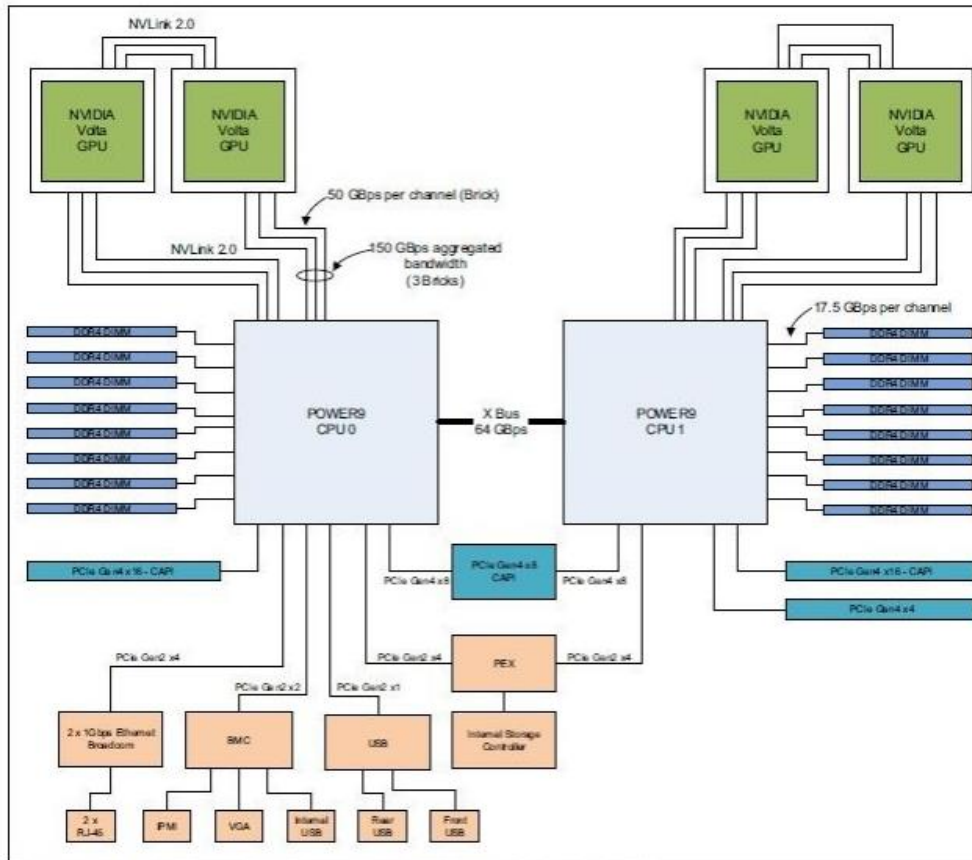


Figure 2-5. The Power AC922 server model GTH logical system diagram

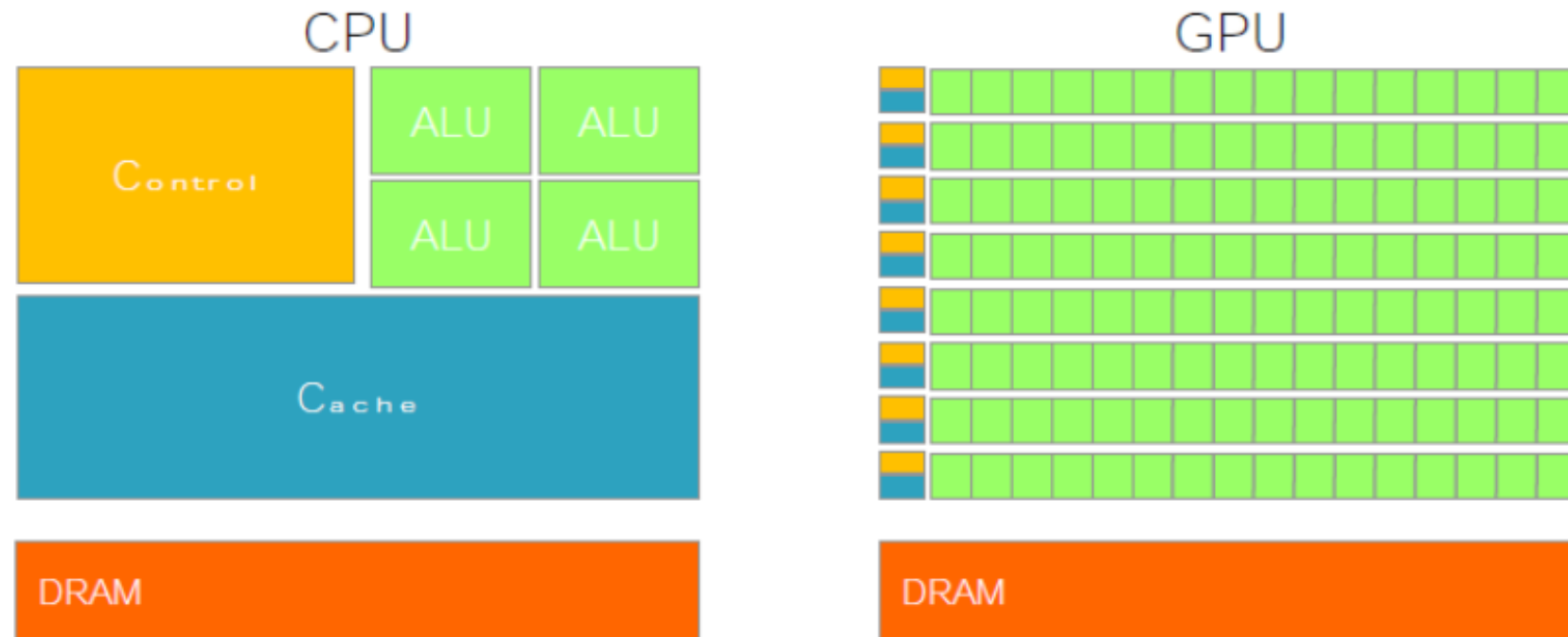
- AC922 “Whiterspoon”
- **32 PFlops peak**
- Nodes: 980 compute + 3 login nodes, 32 TFlops each
- Processors: 2x16 cores IBM 8335-GTG 2.6 (3.1) GHz
- Accelerators: **4xNVIDIA V100 GPUs**, Nvlink 2.0, 16GB
- RAM: 256 GB/node
- Local disk: 1.6TB NVMe
- Internal Network: Mellanox Infiniband EDR DragonFly+
- Disk Space: 8PB storage

# what is a GPU

- Graphic Processing Unit
  - a device equipped with an highly parallel microprocessor(many-core) and a private memory with very high bandwidth
- GPUS are designed to render complex 3D scenes composed of millions of data points/vertex in a very fast frate rate (60/120 FPS)
- the rendering process requires a set of transformations based on linear algebra operations
- the same set of operations are applied on each point of the scene
- each operation is independent with respect to data
- all operations are performed in parallel using a huge number of threads which process all data independently

# what is a GPU

- GPUs are specialized for intense data-parallel computations
- in GPUs more transistors are devoted to data processing rather than data caching and flow control
- main global memory: 32-64GB; high bandwidth: 250-800GB/s

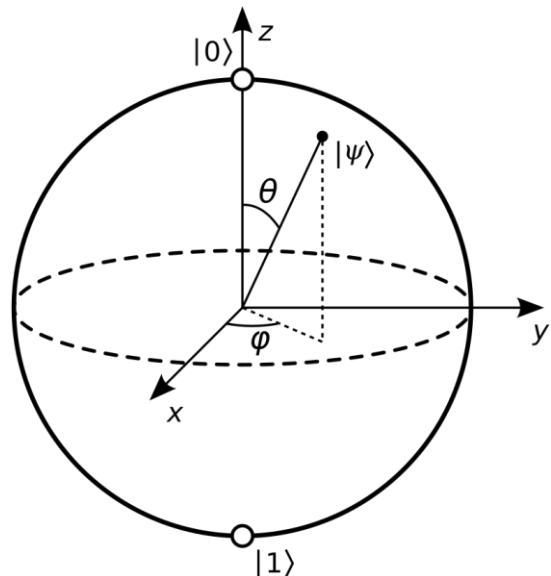


\*ALU=Arithmetic Logic Unit

# Quantum Computing

- a classical bit is a binary digit, either 0 or 1, used to represent information in classical computers;
- A pure qubit state is a coherent superposition of the basis states, I'd write it as  $|\psi\rangle = \alpha|0\rangle + \beta|1\rangle$ , with  $\alpha^2 + \beta^2 = 1$ , it can be represented as a point on the so-called Bloch sphere.
- There are two possible outcomes for the measurement of a qubit—usually taken to have the value "0" and "1", like a bit. However, the general state of a qubit according to quantum mechanics can arbitrarily be a coherent superposition of all computable states simultaneously → possibility to store much more information;
- But a measurement of a qubit would destroy its coherence and irrevocably disturb the superposition state
- Fundamental part of the success would be to harness the process of “quantum entanglement”, but this is rapidly destroyed by noise (produced, for example, by random oscillations of the ions or molecules used as qubits).
- As written in Nature: “Quantum computers: what are they good for? For now, absolutely nothing. But researchers and firms are optimistic about the applications.”

[<https://www.nature.com/articles/d41586-023-01692-9>]



**Bloch sphere** representation of a qubit. In fact, a qubit requires two complex numbers to describe its two probability amplitudes

- Whatever the design, the clever stuff happens when qubits are carefully coaxed into ‘superposition’ states of indefinite character — essentially a mix of digital ones and zeroes.
- Running algorithms on a quantum computer involves directing the evolution of these superposition states. The quantum rules of this evolution allow the qubits to interact to perform computations that are, in practical terms, impossible using classical computers.
- That said, useful computations are possible only on quantum machines with a huge number of qubits, and those do not yet exist. What’s more, qubits and their interactions must be robust against errors introduced through the effects of thermal vibrations, cosmic rays, electromagnetic interference and other sources of noise. These disturbances can cause some of the information necessary for the computation to leak out of the processor, a situation known as decoherence. That can mean dedicating a large proportion of the qubits to error-correction routines that keep a computation on track.

# basics of parallel programming

- OpenMP
- MPI
- simple examples

# OpenMP: De-facto standard for Shared-Memory Parallelization.

## History:

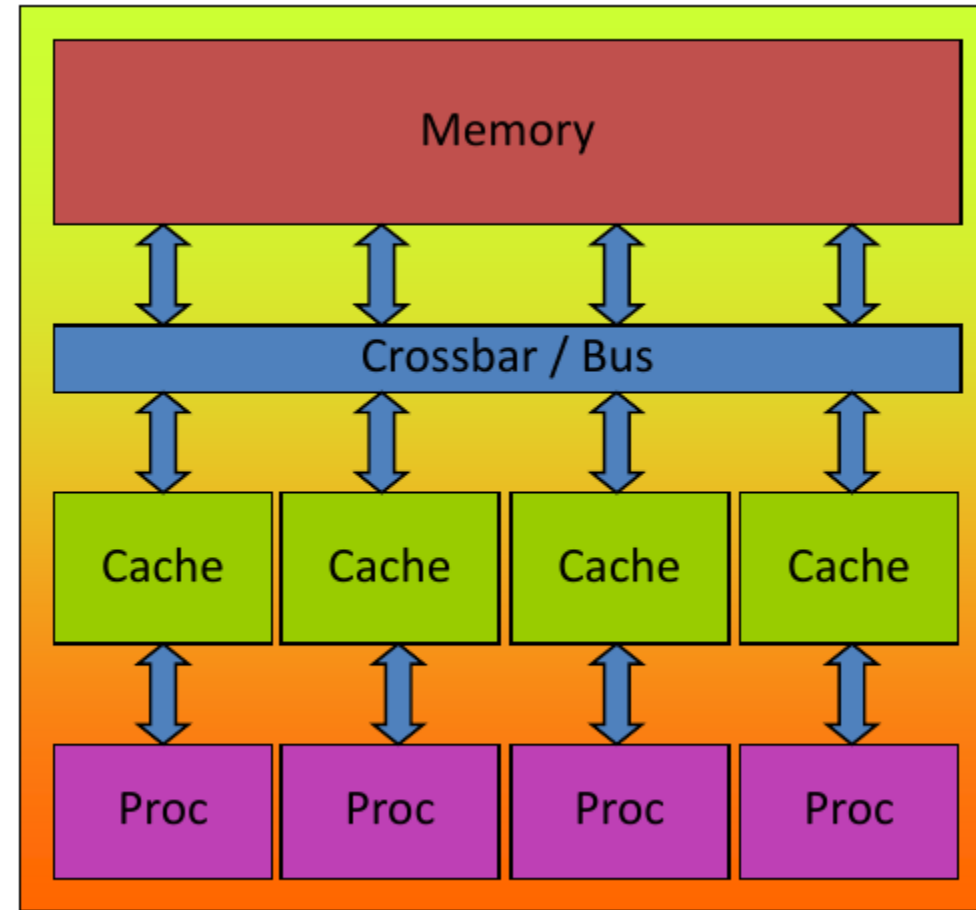
- 1997: OpenMP 1.0 for FORTRAN
- 2000: OpenMP 2.0 for FORTRAN
- 2002: OpenMP 2.0 for C and C++
- 2005: OpenMP 2.5 now includes both programming languages.
- 07/2013: OpenMP 4.0
- 11/2018: OpenMP 5.0
- 11/2020: OpenMP 5.1



- What is OpenMP?
  - Parallel Region & Worksharing
  - Tasking
  - SIMD / Vectorization
  - Accelerator Programming

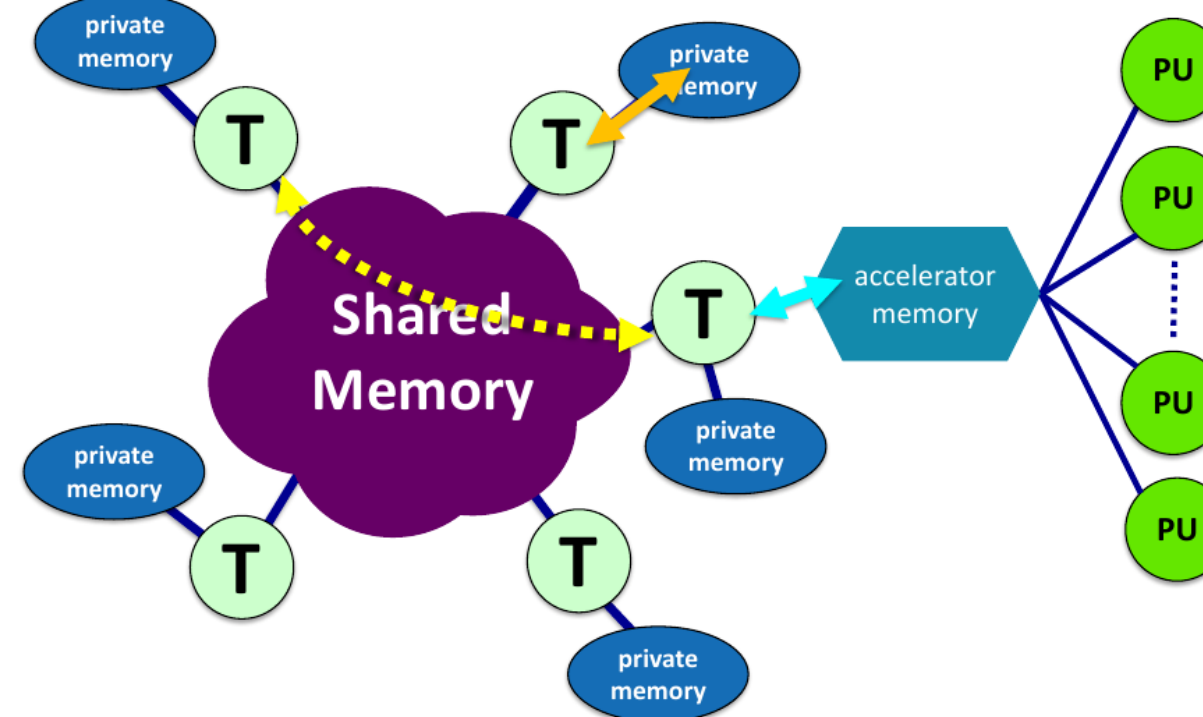
OpenMP: **Shared**-Memory Parallel Programming Model.

- All processors/cores access a shared main memory.
- Real architectures are more complex, as we have seen
- Parallelization in OpenMP employs multiple threads



# The OpenMP Memory Model

- All threads have access to the same, globally shared memory
- Data in private memory is only accessible by the thread owning this memory
- No other thread sees the change(s) in private memory
- Data transfer is through shared memory and is 100% transparent to the application

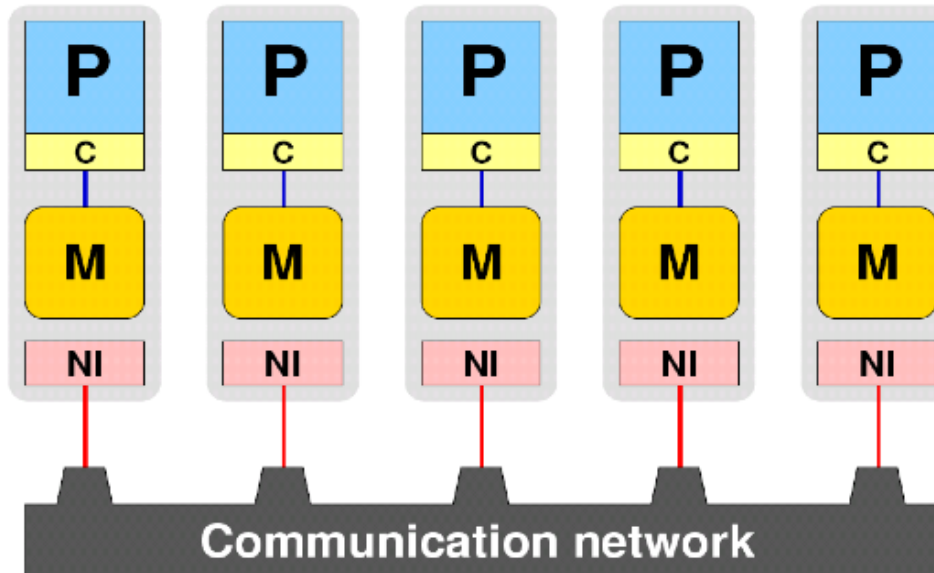


# Message Passing Interface (MPI)

[www.mpi-forum.org/](http://www mpi-forum.org/)

MPI: **Distributed**-Memory Parallel Programming Model.

- processors P do not share any topological entity with each other, they're equal
- Each one has its dedicated memory region (M)
- They are connected using one uniform network (NI)



# Parallel Region and Structured Blocks: simple OpenMP example

- The parallelism has to be expressed explicitly.

C/C++

```
#pragma omp parallel
{
...
structured block
...
}
```

Fortran

```
!$omp parallel
...
structured block
...
!$omp end parallel
```

- Structured Block
  - Exactly one entry point at the top
  - Exactly one exit point at the bottom
  - Branching in or out is not allowed
  - Terminating the program is allowed (abort / exit)

# example1: for worksharing

- OpenMP's most common worksharing construct: for

C/C++

```
int i;
#pragma omp for
for (i = 0; i < 100; i++)
{
    a[i] = b[i] + c[i];
}
```

Fortran

```
INTEGER :: I
!$omp do
DO i = 0, 99
    a[i] = b[i] + c[i]
END DO
```

- Distribution of loop iterations over all threads in a Team.
- Scheduling of the distribution can be influenced.
- Loops often account for most of a program's runtime!

# worksharing illustrated

Pseudo-Code  
Here: 4 Threads

**Serial**

```
do i = 0, 99
  a(i) = b(i) + c(i)
end do
```

**Thread 1**

```
do i = 0, 24
  a(i) = b(i) + c(i)
end do
```

**Thread 2**

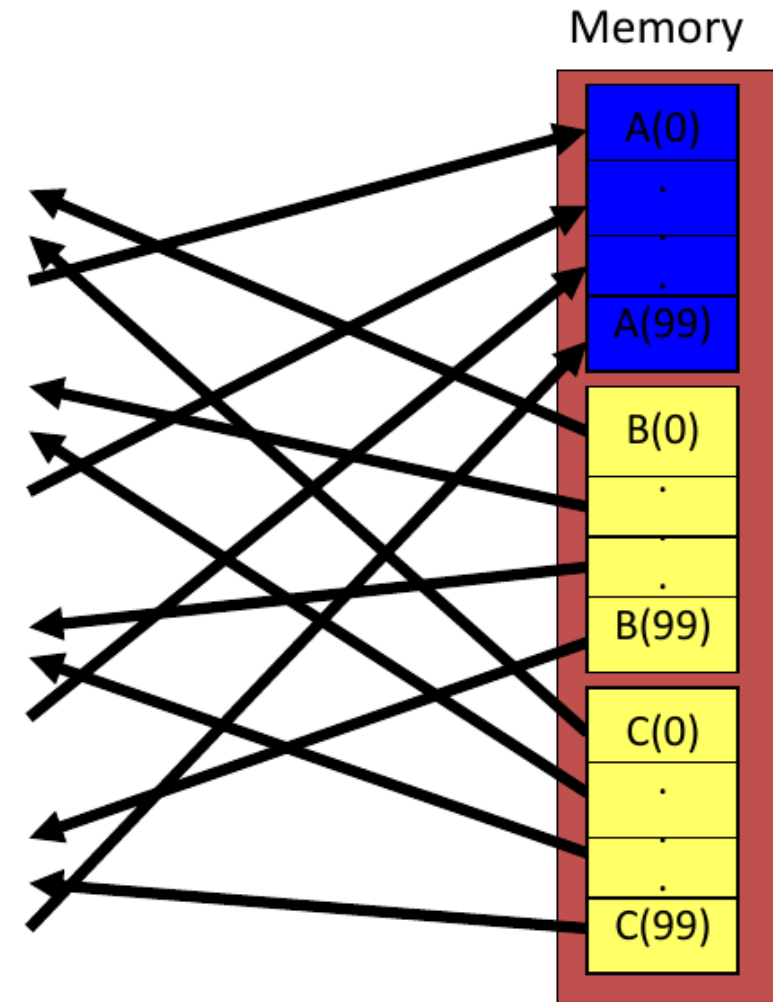
```
do i = 25, 49
  a(i) = b(i) + c(i)
end do
```

**Thread 3**

```
do i = 50, 74
  a(i) = b(i) + c(i)
end do
```

**Thread 4**

```
do i = 75, 99
  a(i) = b(i) + c(i)
end do
```



## example2: a more insidious for loop

- Can all loops be parallelized with for-constructs? No!
- Simple test: If the results differ when the code is executed backwards, the loop iterations are not independent. BUT: This test alone is not sufficient.

```
C/C++  
int i, int s = 0;  
#pragma omp parallel for  
for (i = 0; i < 100; i++)  
{  
    s = s + a[i];  
}
```

- Data Race: if between two synchronization points at least one thread writes to a memory location from which at least one other thread reads, the result is not deterministic (race condition).

## example2: a more insidious for loop

- A Critical Region is executed by all threads, but by only one thread simultaneously (Mutual Exclusion).

```
C/C++  
int i, s = 0;  
#pragma omp parallel for  
for (i = 0; i < 100; i++)  
{  
    #pragma omp critical  
    { s = s + a[i]; }  
}
```

- Does not scale well!

## example2: a more insidious for loop

- In a reduction-operation the operator is applied to all variables in the list. The variables have to be shared.
  - reduction(operator:list)
  - The result is provided in the associated reduction variable

```
C/C++  
int i, s = 0;  
#pragma omp parallel for reduction(+:s)  
for(i = 0; i < 99; i++)  
{  
    s = s + a[i];  
}
```

# final piece of code: compute $\pi$

```

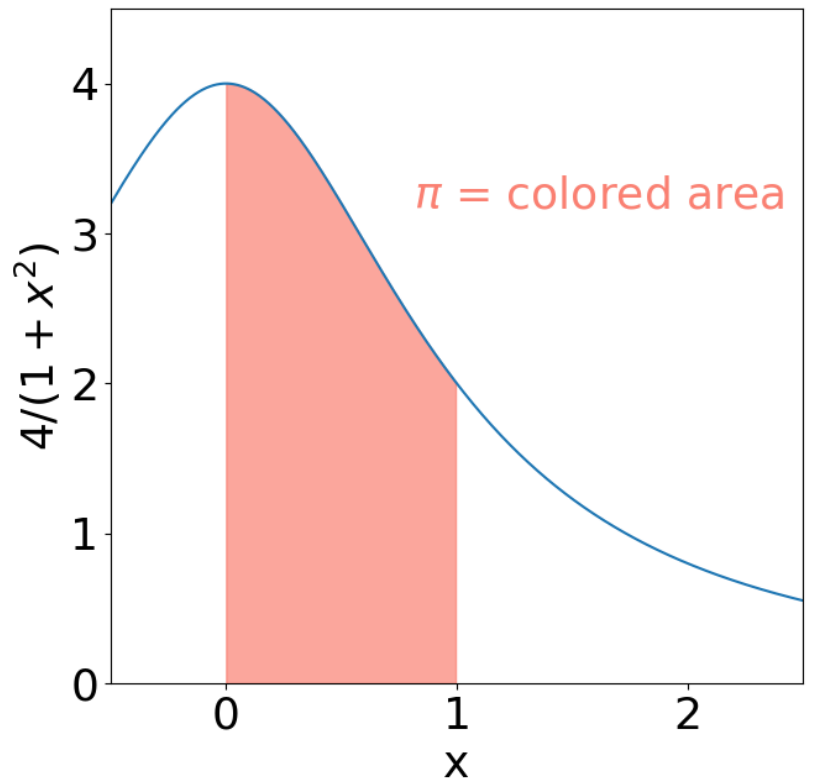
double f(double x)
{
    return (4.0 / (1.0 + x*x));
}

double CalcPi (int n)
{
    const double fH = 1.0 / (double) n;
    double fSum = 0.0;
    double fX;
    int i;

#pragma omp parallel for private(fX,i)
reduction(+:fSum)
    for (i = 0; i < n; i++)
    {
        fX = fH * ((double)i + 0.5);
        fSum += f(fX);
    }
    return fH * fSum;
}

```

$$\pi = \int_0^1 dx \frac{4}{1+x^2}$$



# how to work in an HPC infrastructure

- first you need to get some computational time, typically through a call for the use of resources;
- when you enter you find yourself in a LINUX environment

```
aurelio@rat2$ marconi
Last login: Tue Mar  7 15:19:16 2023 from 150.178.101.4
*****
* Welcome to MARCONI /
*      MARCONI-fusion @ CINECA - NeXtScale cluster - CentOS 7.3
*
* SKL partition - 3124 nodes with:
*   - 2*24-core Intel Xeon 8160 CPU @ 2.10GHz
*   - 192 GB DDR4 RAM
*
* Intel OmniPath (100Gb/s) high-performance network
* SLURM 22.05
*
* For a guide on Marconi:
* wiki.u-gov.it/confluence/display/SCAIUS/UG3.1%3A+MARCONI+UserGuide
* For support: superc@cineca.it
*****
IN EVIDENCE:
- An automatic cleaning procedure for the $CINECA_SCRATCH is active, each day
  all files older than 40 days will be cancelled.
- The "module" environment is installed and based on profiles. Use the modmap
  command to identify the correct profile ("modmap -h" for help).
[/marconi_work/FUA37_PIXIE3D/.veranda/nemato.1.6.3/runs/lcs-tool]
maurelio@r000u06l01$
```

# how to work in an HPC infrastructure: the module system

- The **module system** is a concept available on most supercomputers,
- In most cases, a **supercomputer has far more software installed than the average user will ever use**. Each of these software packages need different settings in terms of \$PATH, \$LD\_LIBRARY\_PATH and other environment variables, which can adversely affect each other or even be mutually exclusive.
- Therefore, **the settings for all these software packages and their supported versions are encapsulated in “environment modules”** maintained by the module system.
- By means of the module system, all software currently available on your cluster can be listed, loaded, and unloaded, by using the command module.

[on Marconi HPC] use `module avail` to see all the available modules

# result of the module avail command

```
maurelio@r000u06l01$ module avail
----- /cineca/prod/opt/modulefiles/profiles -----
profile/advanced profile/base profile/cheese profile/eng profile/knl profile/phys profile/unstable
profile/archive profile/bioinf profile/chem profile/global profile/lifesc profile/statistics
profile/astro profile/candidate profile/deeplrn profile/global_prove profile/neurosc profile/superc

----- /cineca/prod/opt/modulefiles/base/environment -----
autoload env-bdw/1.0 env-knl/1.0 env-skl/1.0 prace/1.0

----- /cineca/prod/opt/modulefiles/base/libraries -----
2decomp_fft/1.5.847--intelmpi--2018--binary matheval/1.1.11--intelmpi--2018--binary parmetis/4.0.3--intelmpi--2018--binary zlib/1.2.8--gnu--6.1.0
blas/3.8.0--intel--pe-xe-2018--binary metis/5.1.0--intel--pe-xe-2018--binary petsc/3.13.3--intelmpi--2018--binary zlib/1.2.11--gnu--8.3.0
boost/1.58--intelmpi--2018--binary mkl/2018--binary petsc/3.13.3_complex--intelmpi--2018--binary
boost/1.66.0--intelmpi--2018--binary mkl/2020--binary petsc/3.13.3_int64--intelmpi--2018--binary
boost/1.78.0--intelmpi--2018--binary mpi4py/3.0.0--python--3.6.4 petsc/3.16.0--intelmpi--2020--binary
cubelib/4.4--intelmpi--2018--binary nag/mark26--binary petsc/3.16.0_complex--intelmpi--2020--binary
cubelib/4.7--intelmpi--2020--binary nag/mark27--binary pnetcdf/1.11--intelmpi--2018--binary
fftw/3.3.5--intelmpi--2017--binary netcdf-cxx4/4.3.0--intel--pe-xe-2018--binary proj/8.0--intel--pe-xe-2018--binary
fftw/3.3.7--intelmpi--2018--binary netcdf-cxx4/4.3.0--intelmpi--2018--binary qt/5.7.0--intelmpi--2018--binary
fftw/3.3.8--intelmpi--2020--binary netcdf/4.6.1--intel--pe-xe-2018--binary qt/5.9.0--gnu--6.1.0
gdal/3.2.2--intel--pe-xe-2018--binary netcdf/4.6.1--intelmpi--2018--binary scalapack/2.0.2--intelmpi--2018--binary
geos/3.9.1--intel--pe-xe-2018--binary netcdf/4.9.0--intel--pe-xe-2020--binary scipy/1.2.2--python--2.7.12
gsl/2.5--intel--pe-xe-2018--binary netcdf/4.9.0--intelmpi--2020--binary scipy/1.2.2--python--3.6.4
gts/0.7.6 netcdff/4.4.4--intel--pe-xe-2018--binary slepc/3.13.3--intelmpi--2018--binary
hdf5/1.8.18--intel--pe-xe-2018--binary netcdff/4.4.4--intelmpi--2018--binary slepc/3.13.3_int64--intelmpi--2018--binary
hdf5/1.8.18--intelmpi--2018--binary netcdff/4.6.0--intel--pe-xe-2020--binary szip/2.1--gnu--6.1.0
hdf5/1.10.4--intel--pe-xe-2018--binary netcdff/4.6.0--intelmpi--2020--binary szip/2.1.1--gnu--8.3.0
hdf5/1.10.4--intelmpi--2018--binary numpy/1.14.0--python--2.7.12 udunits/2.2.28--intel--pe-xe-2018--binary
```

# result of the module avail command

- and the rest is up to your practice. but in case you're experiencing an issue ask me and I may help.

```
maurelio@r000u06l01$ module avail
----- /cineca/prod/opt/modulefiles/profiles -----
profile/advanced profile/base profile/cheese profile/eng profile/knl profile/phys profile/unstable
profile/archive profile/bioinf profile/chem profile/global profile/lifesc profile/statistics
profile/astro profile/candidate profile/deeplrn profile/global_prove profile/neurosc profile/superc

----- /cineca/prod/opt/modulefiles/base/environment -----
autoload env-bdw/1.0 env-knl/1.0 env-skl/1.0 prace/1.0

----- /cineca/prod/opt/modulefiles/base/libraries -----
2decomp_fft/1.5.847--intelmpi--2018--binary matheval/1.1.11--intelmpi--2018--binary parmetis/4.0.3--intelmpi--2018--binary zlib/1.2.8--gnu--6.1.0
blas/3.8.0--intel--pe-xe-2018--binary metis/5.1.0--intel--pe-xe-2018--binary petsc/3.13.3--intelmpi--2018--binary zlib/1.2.11--gnu--8.3.0
boost/1.58--intelmpi--2018--binary mkl/2018--binary petsc/3.13.3_complex--intelmpi--2018--binary
boost/1.66.0--intelmpi--2018--binary mkl/2020--binary petsc/3.13.3_int64--intelmpi--2018--binary
boost/1.78.0--intelmpi--2018--binary mpi4py/3.0.0--python--3.6.4 petsc/3.16.0--intelmpi--2020--binary
cubelib/4.4--intelmpi--2018--binary nag/mark26--binary petsc/3.16.0_complex--intelmpi--2020--binary
cubelib/4.7--intelmpi--2020--binary nag/mark27--binary pnetcdf/1.11--intelmpi--2018--binary
fftw/3.3.5--intelmpi--2017--binary netcdf-cxx4/4.3.0--intel--pe-xe-2018--binary proj/8.0--intel--pe-xe-2018--binary
fftw/3.3.7--intelmpi--2018--binary netcdf-cxx4/4.3.0--intelmpi--2018--binary qt/5.7.0--intelmpi--2018--binary
fftw/3.3.8--intelmpi--2020--binary netcdf/4.6.1--intel--pe-xe-2018--binary qt/5.9.0--gnu--6.1.0
gdal/3.2.2--intel--pe-xe-2018--binary netcdf/4.6.1--intelmpi--2018--binary scalapack/2.0.2--intelmpi--2018--binary
geos/3.9.1--intel--pe-xe-2018--binary netcdf/4.9.0--intel--pe-xe-2020--binary scipy/1.2.2--python--2.7.12
gsl/2.5--intel--pe-xe-2018--binary netcdf/4.9.0--intelmpi--2020--binary scipy/1.2.2--python--3.6.4
gts/0.7.6 netcdff/4.4.4--intel--pe-xe-2018--binary slepc/3.13.3--intelmpi--2018--binary
hdf5/1.8.18--intel--pe-xe-2018--binary netcdff/4.4.4--intelmpi--2018--binary slepc/3.13.3_int64--intelmpi--2018--binary
hdf5/1.8.18--intelmpi--2018--binary netcdff/4.6.0--intel--pe-xe-2020--binary szip/2.1--gnu--6.1.0
hdf5/1.10.4--intel--pe-xe-2018--binary netcdff/4.6.0--intelmpi--2020--binary szip/2.1.1--gnu--8.3.0
hdf5/1.10.4--intelmpi--2018--binary numpy/1.14.0--python--2.7.12 udunits/2.2.28--intel--pe-xe-2018--binary
```

questions?



- for any question mail to:

[marco.veranda@igi.cnr.it](mailto:marco.veranda@igi.cnr.it)



# Spare:

# magnetic islands. The helical flux function

- Let us consider a magnetic field  $\mathbf{B}(r)$  in a three-dimensional space with a curvilinear coordinate system whose coordinates are labeled as  $u_i = (u_1, u_2, u_3)$ .
- Let us suppose that the system has a symmetry, i.e.,  $\frac{\partial}{\partial u_3} = 0$ .
- The magnetic field can be written using the vector potential  $\mathbf{A}(r)$  as:  $\mathbf{B} = \nabla \times \mathbf{A} = \frac{\epsilon_{ijk}}{J} \frac{\partial A_j}{\partial u^i} \mathbf{e}_k$ , where  $\epsilon_{ijk}$  represents the Levi-Civita tensor,  $J$  the Jacobian of the coordinate transformation,  $A_j$  the covariant component of the vector potential and  $\mathbf{e}_k$  is the covariant basis vector.
- Imposing the relation  $\mathbf{B} \cdot \nabla \chi = 0$ , choosing a gauge  $A_1 = 0$  and remembering that  $\frac{\partial}{\partial u_3} = 0$  it is found that:

$$\frac{\partial A_3}{\partial u^2} \frac{\partial \chi}{\partial u^1} - \frac{\partial A_3}{\partial u^1} \frac{\partial \chi}{\partial u^2} = 0, \text{ meaning that the equality is satisfied if}$$

$$\chi = A_3 = \mathbf{A} \cdot \mathbf{e}_3$$

- In cylindrical geometry + choosing the most general symmetry in 2D (the helical one) we get  $A_3 = \chi = mA_z - \frac{n}{R_0} r A_\theta$